We are IntechOpen, the world's leading publisher of Open Access books Built by scientists, for scientists

6,900
Open access books available

186,000
International authors and editors

200M
Downloads

Our authors are among the

154
Countries delivered to

TOP 1%
most cited scientists

12.2%
Contributors from top 500 universities

CLARIVATE ANALYTICS
BOOK CITATION INDEX
INDEXED

WEB OF SCIENCE™

Selection of our books indexed in the Book Citation Index
in Web of Science™ Core Collection (BKCI)

Interested in publishing with us?
Contact book.department@intechopen.com

Numbers displayed above are based on latest data collected.
For more information visit www.intechopen.com

Chapter

Low-Specificity and High-Sensitivity Immunostaining for Demonstrating Pathogens in Formalin-Fixed, Paraffin-Embedded Sections

Yutaka Tsutsumi

Abstract

The present review describes a part of the author's own experience in applying immunoperoxidase staining to routine histopathological diagnosis. The target disorder was focused on infection. In the practice of pathology diagnosis services, it is important for us diagnostic pathologists to judge whether the lesion is caused by an infection or not. When an infectious disease is highly likely, the visualization of pathogens within the inflammatory lesion is required to suggest a causative agent. Two main approaches the author would like to introduce include (1) the use of commercially available antisera showing wide cross-reactivity to a variety of bacteria and (2) the use of diluted patients' sera. These immunohistochemical studies employing "low-specificity" and "high-sensitivity" probes are useful for confirming the localization of pathogen within the infectious lesion.

Keywords: infectious diseases, diagnostic immunohistochemistry, specificity, sensitivity, commercial antiserum, patient's serum, paraffin section

1. Introduction

Infectious diseases kill a significant number of people in the world. Of the top 10 leading causes of death in low-income countries in 2016, pneumonia, diarrheal diseases, acquired immune deficiency syndrome (AIDS), malaria, and tuberculosis are listed up. More than half of deaths in low-income countries were due to communicable diseases, maternal causes, conditions arising during pregnancy and childbirth, and nutritional deficiencies, while such causes shared less than 7% of deaths in high-income countries [1]. It is no double to say that the detection of infectious agents in the lesion is essential for the histopathological diagnosis of infectious diseases [2, 3]. For the correct diagnosis and appropriate treatment of the patient, immunohistochemical demonstration of pathogens within the lesion must be suitable and desirable [4–10].

Needless to say, the most important factor, the "life," in the immunohistochemical analysis should be a high-specificity antibody for exactly demonstrating the corresponding antigen. A variety of immunohistochemical techniques for

increasing the sensitivity of detection have been developed, in order to localize the antigens under highly specific and highly sensitive conditions in routinely processed (formalin-fixed, paraffin-embedded) sections [11–13]. Immunohistochemical approach is quite fitted to the histopathological diagnosis of infectious diseases, since the antigens of the pathogen are absent from the human tissue specimens [4, 7–10].

However, pathogens express multiple antigens, and the antigens are often cross-reactive among different pathogens [14]. The pathogen in a single category further reveals a variety of serum types [15]. It is more difficult for us pathologists than expected to detect a certain pathogen using a single antibody [4, 7]. It is next to impossible to prepare and keep specific antibodies in hand for immunohistochemical diagnosis in a single institution simply because there are too many species of microbes pathogenic to humans. We have a limited number of commercially available antibodies against pathogens. Useful commercial antibodies may soon disappear from the market because of a simple reason: the dead stock [16].

In the routine practice of histopathological services using hematoxylin and eosin (H&E) staining, it is often the situation that the pathologists are requested to judge if the lesion is infective or not. Namely, the presence of some sort of pathogenic organisms within the lesion should be shown with the maximal priority in making the diagnosis, and the detailed identification of the species name should be analyzed using different technologies afterward. For example, if a lesion showing massive necrosis is experienced, we must comment that the necrosis is infective in origin or tumor-related. In such a situation, an antibody widely cross-reactive to bacteria but unreactive to human tissue is valuable. A monoclonal antibody H9 (a gift of Prof. Shigeru Kamiya, Department of Microbiology, Kyorin University School of Medicine, Mitaka, Tokyo) against bacteria-specific heat shock protein (HSP)-60, not cross-reactive animal mitochondrial HSP-60, is quite valuable [7, 17], but it is not commercially available. Lipopolysaccharide (LPS) or endotoxin, located in the outer layer of the bacterial wall, should be the good marker of Gram-negative bacteria (refer to **Figure 11**) [18], but it is practically difficult for us to get a monoclonal or polyclonal antibody detecting widely cross-reactive LPS.

In order to visualize pathogens in formalin-fixed, paraffin-embedded sections, we do not necessarily need to prepare antibodies with high specificity [4, 7, 19]. The author routinely uses four kinds of commercially available rabbit antisera raised against *Bacillus* Calmette-Guérin (BCG; *Mycobacterium bovis*), *Bacillus cereus* (*B. cereus*), *Treponema pallidum* (*T. pallidum*), and *Escherichia coli* (*E. coli*) [16, 19]. For immunoperoxidase staining, the amino acid polymer technique or indirect immunoperoxidase method is employed. Immunostaining using these low-specificity antimicrobial antisera commonly yields clear high-sensitivity signals with low background, because of poor cross-reactivity of bacterial antigens to human cells and tissues.

The second approach for detecting unknown pathogens in the histopathological sections is the use of patient's serum [4, 7, 8, 20–23]. Patients' sera diluted at 1:500 or 1:1000 become convenient probes for indirect immunoperoxidase localization of pathogens in formalin-fixed, paraffin-embedded sections, particularly when cellular tissue reactions have been confirmed under the microscope. Serum antibody titer should be high in the recovery or chronic stage of illness. The existence of inflammatory tissue reaction, such as an abscess or granuloma, indicates that immune cells in the patient have been activated against the causative pathogen. The second approach is of high value for protozoan and helminthic disorders.

2. Commercially available antibodies against pathogens: the author's experience

In **Table 1**, commercially available antibodies against pathogens are listed up, simply for the convenience of the readers. The catalog is solely based on the author's experience, so that the antibodies may not be most suitable for detecting pathogens in routinely prepared sections [8, 19]. Some antibodies may be no longer available, simply because of limited market. The specificity of the antibodies is categorized

Pathogen	Type (clone)	Company	Dilution	Pretreatment	Specificity
Antibacterial antibody					
Actinomyces	Mo (396AN1)	DSHB	1:5	CB6	High
Bacillus cereus	Rabbit	Abcam	1:500	CB6	Low
Bartonella henselae	Mo (H2A10)	Biocare	1:100	EDTA	High
BCG	Rabbit	Dako	1:5000	None	Low
Campylobacter jejuni	Mo (4080)	Novocastra	1:50	CB6	Moderate
Chlamydia trachomatis	Mo (B104.1)	Biomeda	1:5	CB6	High
Escherichia coli	Rabbit	Dako	1:20,000	PK	Low
E. coli	Mo (MAB706)	Millipore	1:50	CB6	High
E. coli (LPS)	Mo (2D7/1)	Abcam	1:5000	CB6	Moderate
Enterococcus	Rabbit	Abcam	1:2000	None	Moderate
Helicobacter pylori	Rabbit	Dako	1:50	PK	Moderate
Helicobacter pylori	Mo (UCL3R)	Novocastra	1:100	EDTA	High
Klebsiella pneumoniae	Mo (70–2)	Monosan	1:300	None	High
Legionella pneumophila	Rabbit	Denka Seiken	1:500	EDTA	High
Mycobacterium tuberculosis	Mo (MAB738)	Chemicon	1:3000	EDTA	High
M. tuberculosis (MPT64)	Rabbit	Abcam	1:800	CB6	High
Pneumococcus	Mo (128/390)	Chemicon	1:1000	None	Moderate
Pneumolysin	Mo (9.1/2/3/6)	Novocastra	1:50	EDTA	High
Protein A	Mo (SPA-27)	Sigma	1:100	PK	Moderate
Protein G	Rabbit	Abcam	1:500	PK	Moderate
Pseudomonas aeruginosa	Mo (B11)	Biogenesis	1:800	EDTA	High
Staphylococcus	Mo (STAPH11–248.2)	Chemicon	1:500	PK	Moderate
Streptococcus	Goat	BioReagents	1:500	PK	Moderate
Treponema pallidum	Rabbit	Biocare	1:1000	EDTA	Low
Treponema pallidum	Mo (J010J)	Thermo	1:50	CB6	High
Antifungal antibody					
Aspergillus	Rabbit	Biocare	1:200	EDTA	Moderate

Pathogen	Type (clone)	Company	Dilution	Pretreatment	Specificity
Aspergillus	Mo (WF-AF-1)	Thermo	1:50	EDTA	High
Candida	Rabbit	Unitika	1:8000	PK	Moderate
Candida	Mo (MaB806)	Chemicon	1:400	Pepsin	High
Cryptococcus	Rabbit	Dako	1:500	None	Moderate
Pneumocystis	Mo (3F6)	Dako	1:100	CB6	High
Rhizopus	Mo (WSSA-RA-1)	Thermo	1:50	CB6	High
Antiviral antibody					
Adenovirus	Mo (M58 + M73)	Abcam	1:400	PK	High
BK virus	Mo (5E6)	Abnova	1:500	CB6	High
Cytomegalovirus	Mo (CCH2 + DDG9)	Dako	1:200	EDTA	High
EB virus (LMP1)	Mo (CS1–CS4)	Dako	1:50	PK	High
EB virus (EBNA2)	Mo (PE2)	Dako	1:100	EDTA	High
Influenza virus A	Mo (1331)	AbD	1:100	PK	High
Influenza virus A	Mo (1A52.9)	Acris	1:100	PK	High
Influenza virus B	Guinea pig	Denka Seiken	1:100	EDTA	High
HBs antigen	Goat	Bioss	1:2000	PK	High
HBs antigen	Mo (HB-024)	Japan Biotest	1:500	None	High
HBc antigen	Rabbit	Dako	1:15,000	EDTA	High
HBe antigen	Mo (BE-05)	Institute of Immunology	1:50	PK	High
HCV (NS3–NS4)	Mo (Tordji-22)	Signet	1:200	EDTA	High
HCV (NS3)	Mo (MMM33)	Novocastra	1:100	CB7	High
HCV (NS4)	Mo (5D4-10E7)	Abcam	1:300	EDTA	High
HCV (NS5a)	Mo (7-D4)	Fitzgerald	1:100	EDTA	High
HCV (core)	Mo (Aa70–Aa90)	Chemicon	1:100	EDTA	High
Herpes simplex virus-1	Rabbit	Dako	1:500	None	Moderate
Herpes simplex virus-2	Rabbit	Dako	1:1500	None	Moderate
HIV (p24)	Mo (kal-1)	Dako	1:1000	EDTA	High
HPV	Mo (K1H8)	Dako	1:500	CB6	High
HPV16	Mo (CamVir-1)	BioGenex	1:5000	EDTA	High
JC virus	Rabbit	Dako	1:300	CB7	High
Merkel cell polyomavirus	Mo (CM2B4)	Santa Cruz	1:100	EDTA	High
Measles virus	Rabbit	Novus	1:1000	EDTA	High
Mumps virus	Mo (MAB846)	Chemicon	1:400	EDTA	High
Norovirus (GII/4)	Rabbit	Denka Seiken	1:500	None	High
Parvovirus B19	Mo (R92.2.8)	Novocastra	1:1000	EDTA	High
RS virus	Mo (603705)	Novocastra	1:200	EDTA	High

Pathogen	Type (clone)	Company	Dilution	Pretreatment	Specificity
SV40 (T-antigen)	Mo (PAb416)	Millipore	1:100	EDTA	High
VZV	Mo (C90.2.8)	Novocastra	1:100	None	High
Antiprotozoan antibody					
Toxoplasma gondii	Rabbit	Abcam	1:200	CB6	High

Abbreviations: *Mo, monoclonal antibody; PK, proteinase K; CB6, citrate buffer at pH 6 (heating); CB7, citrate buffer at pH 7 (heating); EDTA, ethylenediaminetetraacetic acid at pH 8 (heating); DSHB, Developmental Studies Hybridoma Bank; BCG, Bacillus Calmette-Guérin; EB, Epstein-Barr; HB, hepatitis B; HCV, hepatitis C virus; HIV, human immunodeficiency virus; HPV, human papillomavirus; RS, respiratory syncytial; SV40, simian virus 40; VZV, varicella-zoster virus*
Antimicrobial antibodies the author is using are listed up for the readers' convenience.

Table 1.
List of commercially available antibodies against pathogens: the author's experience.

into three grades: high, moderate, and low. Even when we use the high-specificity antibody for immunostaining, careful judgment is requested for the final identification of the causative microbe.

3. Application of commercially available antisera against BCG, *B. cereus*, *T. pallidum*, and *E. coli*

Immunoperoxidase application using four kinds of commercially available rabbit antisera raised against BCG, *B. cereus*, *T. pallidum*, and *E. coli* is described [4, 7, 8, 16, 19]. In this section, immunostaining application to mycobacterial infection, *B. cereus* pneumonia, syphilitic lesions, and *E. coli* infections is described. Although the specificity of the antisera is low, as described below, the respective causative pathogens were clearly demonstrated within the lesions.

3.1 Immunostaining for mycobacterial infections using BCG antiserum

Indirect immunoperoxidase staining using BCG rabbit antiserum (Dako/Agilent Technologies) diluted at a 1:5000 was highly sensitive for detecting mycobacteria in histopathological sections [4, 7, 8, 24, 25]. No pretreatment for antigen retrieval was given. Mycobacterial antigens were clearly demonstrable not only in caseous necrosis in active tuberculosis but also in a fibrous nodule of old calcified tuberculosis (**Figure 1**). BCG antigens were scarcely detectable in epithelioid granulomas. The BCG immunostaining was much more sensitive to detect mycobacteria than conventional acid-fast (Ziehl-Neelsen) staining, as indicated in **Table 2** [4, 24]. In BCG immunostaining, the judgment of positivity can be done easily and quickly, while it takes minutes or longer in case of conventional acid-fast staining. It is evident that the antiserum is reactive with mycobacterial antigenic substances on destroyed bacterial fragments. The BCG immunostaining was also applicable to demonstrating non-tuberculous mycobacteria and *Mycobacterium leprae*. **Figure 2** illustrates positive findings in opportunistic *Mycobacterium avium-intracellulare* (MAI) infection in AIDS and in lepromatous (multibacillary) leprosy in a biopsied skin lesion. No positivity was seen in tuberculoid (paucibacillary) leprosy.

The BCG antigens were extremely stable after prolonged fixation in formalin for a long period of time [19, 26]. **Figure 3** displays dense-positive signals in an exudative pulmonary tuberculosis lesion fixed in formalin for nearly 70 years.

3.2 Immunostaining for *B. cereus* pneumonia using *B. cereus* antiserum

B. cereus pneumonia is characterized by a lethal necrotic and hemorrhagic lesion infrequently seen in an immunocompromised or immunocompetent patient [27]. The autopsied lung was obtained from a female aged 60's long suffering from chronic lymphoplasmacytic leukemia. Gram-positive bacilli with spore formation
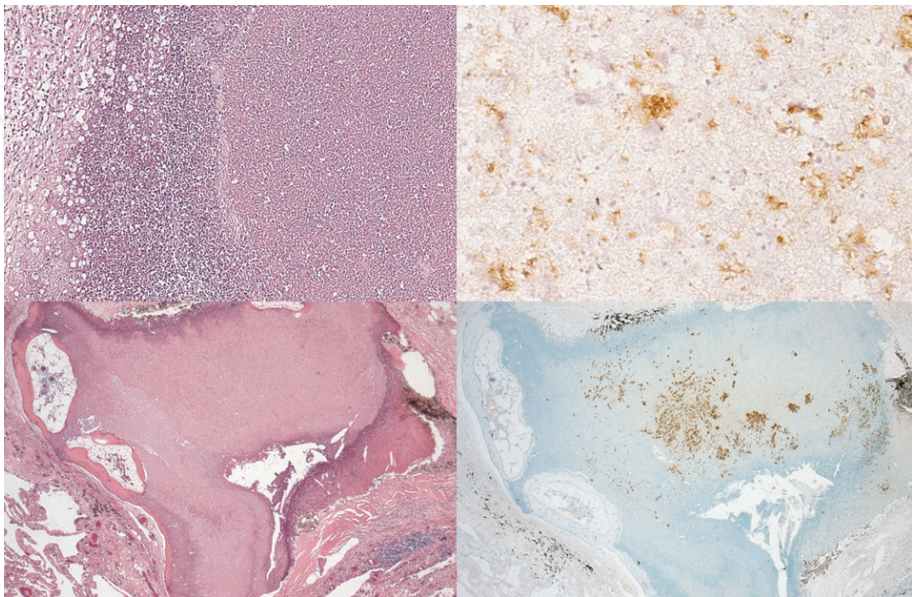

Figure 1.
BCG immunostaining I (upper panels, cerebral tuberculoma; lower panels, old calcified nodule in the lung; left, H&E; right, BCG immunostaining). Mycobacterial antigens were clearly demonstrable not only in caseous necrosis but also in a fibrous nodule of old tuberculosis. Mycobacterial antigenic substances on destroyed bacterial fragments are detectable by the antiserum.

Disease	Acid-fast staining	BCG immunostaining
Tuberculosis		
Exudative lesion	5/6 (83%)	6/6 (100%)
Caseous granuloma	3/11 (27%)	5/11 (45%)
Non-caseous granuloma	0/6 (0%)	1/6 (17%)
Encapsulated caseous focus, non-calcified	0/9 (0%)	5/9 (56%)
Encapsulated caseous focus, calcified	0/11 (0%)	8/11 (73%)
Fibrous focus, calcified	0/1 (0%)	1/1 (100%)
Total	*8/44 (18%)*	*26/44 (59%)*
Leprosy		
Lepromatous leprosy (multibacillary form)	2/2 (100%)[*]	2/2 (100%)
Tuberculoid leprosy (paucibacillary form)	0/3 (0%)	0/3 (0%)
Sarcoid-type granuloma		
Sarcoidosis	0/7 (0%)	0/7 (0%)
Sarcoid-like reaction in lymph node	0/3 (0%)	0/3 (0%)

[*]*Fite modification employing oil-xylene for deparaffinization required.*
Acid-fast staining and BCG immunostaining were compared using three types of granulomatous lesions embedded in paraffin.

Table 2.
Comparative detectability of mycobacteria with acid-fast staining and immunostaining for BCG antigens.
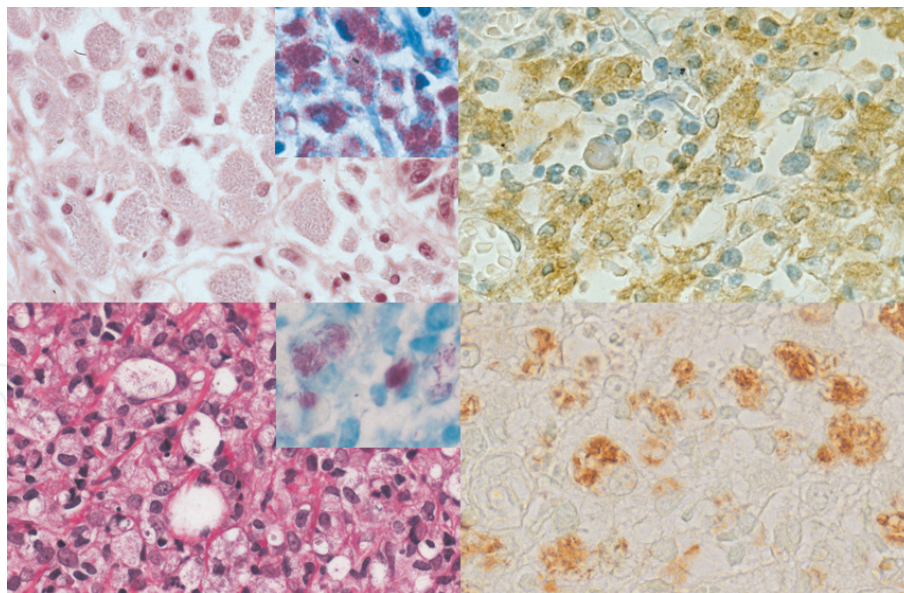
Figure 2.
BCG immunostaining II (upper panels, non-tuberculous mycobacterial lymphadenitis in AIDS; lower panels, lepromatous leprosy; left, H&E; right, BCG immunostaining; inset, acid-fast staining). Striated histiocytes in Mycobacterium avium-intracellulare *(MAI) infection in AIDS and globi in lepromatous (multibacillary) leprosy in a biopsied skin lesion are strongly labeled. Fite modification of acid-fast staining is requested for demonstrating* M. leprae.
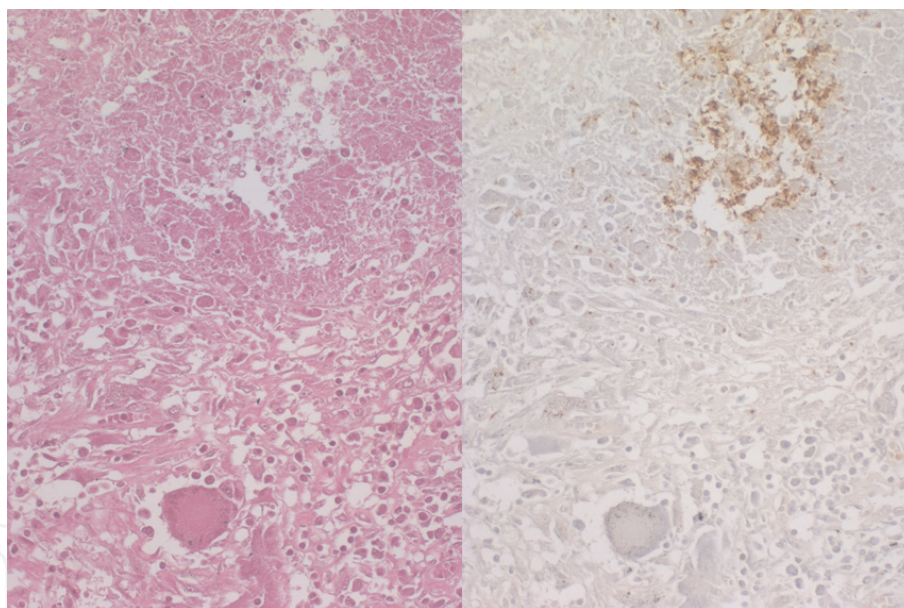

Figure 3.
BCG immunostaining III (left, HE; right, BCG immunostaining). BCG antigens are very stable against fixation. Dense-positive signals are seen in a pulmonary exudative tuberculosis lesion fixed in formalin for 70 years. Of note is that the nuclei are poorly stained with hematoxylin due to prolonged fixation.

were multifocally clustered in the necrohemorrhagic lesion. Immunostaining (the amino acid polymer method, Simple Stain-Max, Nichirei, Tokyo, Japan) using *B. cereus* rabbit antiserum (Abcam) diluted at 1:500 after heat-induced antigen retrieval in 10 mM citrate buffer, pH 6, demonstrated positive signals on the spore of the bacilli (**Figure 4**) [8, 19, 28]. Similar findings were obtained in case of opportunistic soft tissue gangrene caused by *B. cereus* [9].

3.3 Immunostaining for syphilitic lesions using *T. pallidum* antiserum

Warthin-Starry's silver method is technically difficult, frequently with a false-negative result in case of treponemal infection. In contrast, immunostaining

(Simple Stain-Max, Nichirei) using *T. pallidum* rabbit antiserum (Biocare) diluted at 1:1000, after heat-induced antigen retrieval in 1 mM EDTA solution, pH 8, is highly sensitive and reproducible in demonstrating long coiled microbes among the lesion [4, 7–10, 19]. **Figure 5** illustrates a neck skin papule richly infiltrated by plasma cells, biopsied from a middle-aged Japanese male patient in a remission state of malignant lymphoma 2 years after chemotherapy. Clinicians suspected of skin recurrence of malignancy, but immunostaining clearly demonstrated dense infection of coiled bacteria in the epidermis. Plasma cell-rich appearance microscopically suggested the possibility of syphilis, and thus immunostaining for *T. pallidum* was
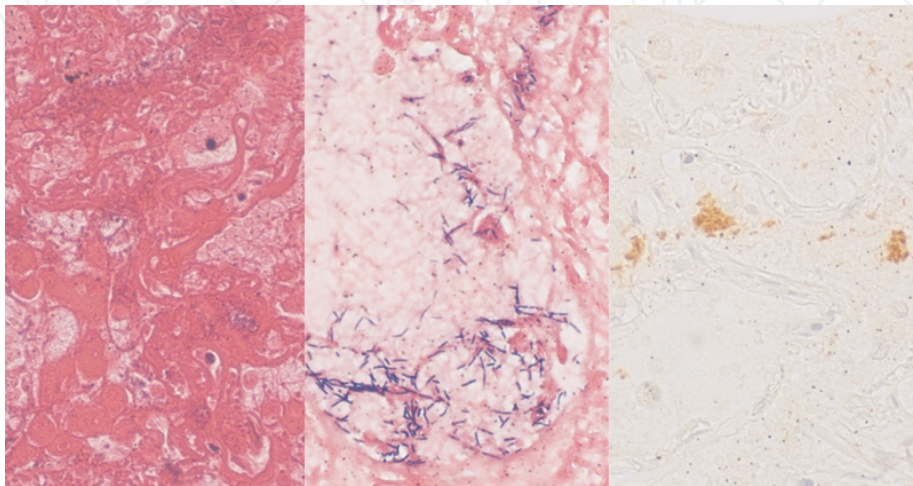
Figure 4.
Lethal B. cereus *pneumonia (left, H&E; center, Gram stain; right, immunostaining using* B. cereus *rabbit antiserum). Gram-positive rods are clustered in the necrohemorrhagic lung tissue, and* B. cereus *antigens are localized in the spore of the bacteria.*
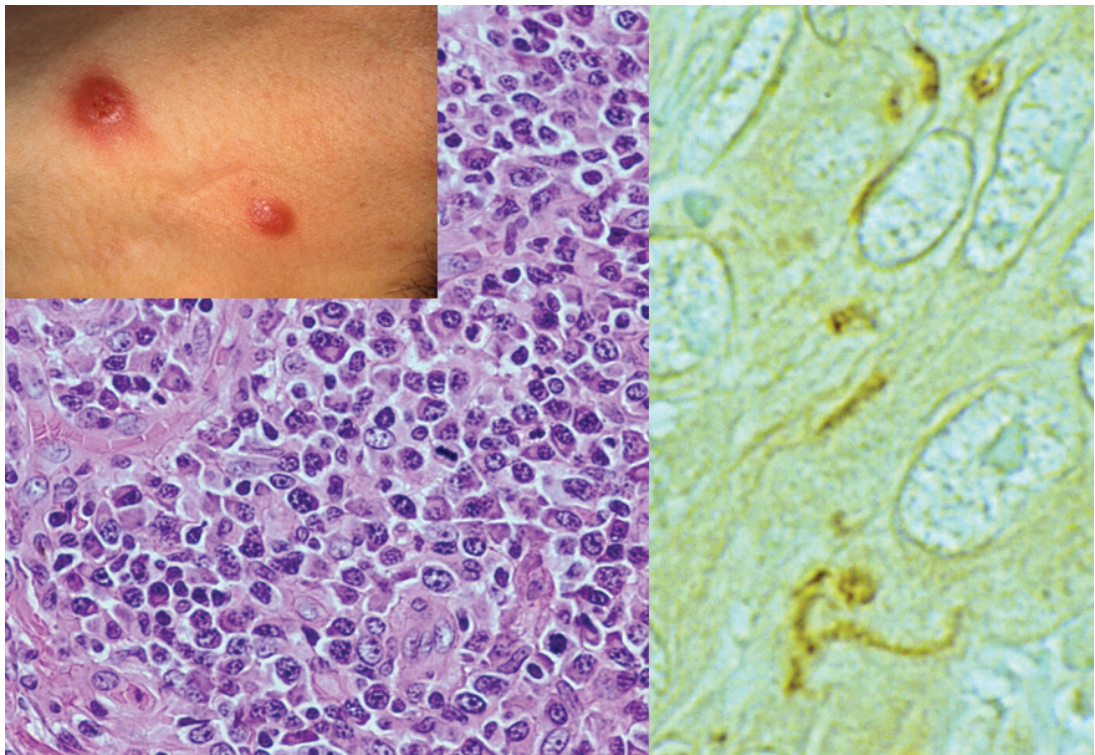
Figure 5.
T. pallidum *immunostaining I (left, H&E; right, immunostaining using* T. pallidum *antiserum; inset, gross appearance of skin eruption on the neck). The papular skin lesion in a middle-aged male is richly infiltrated by plasma cells, and thus the possibility of syphilis was suspected histopathologically. Immunostaining discloses infection of spiral-shaped long bacteria in the epidermis, confirming the diagnosis of clinically unsuspected syphilis.*

performed. The diagnosis of stage II syphilis was subsequently confirmed by serological test for syphilis.

In **Figure 6**, a biopsied penile lesion with painless ulceration (chancre) in stage I and excised syphilitic granulomatous lymphadenitis in stage III are presented. In the penis, numerous spiral microbes were clustered mainly in the basal part of the squamous mucosa and around the dermal capillary vessels. In the stage III lesion with granulomatous reaction, coiled spirochetes were infrequently observed.
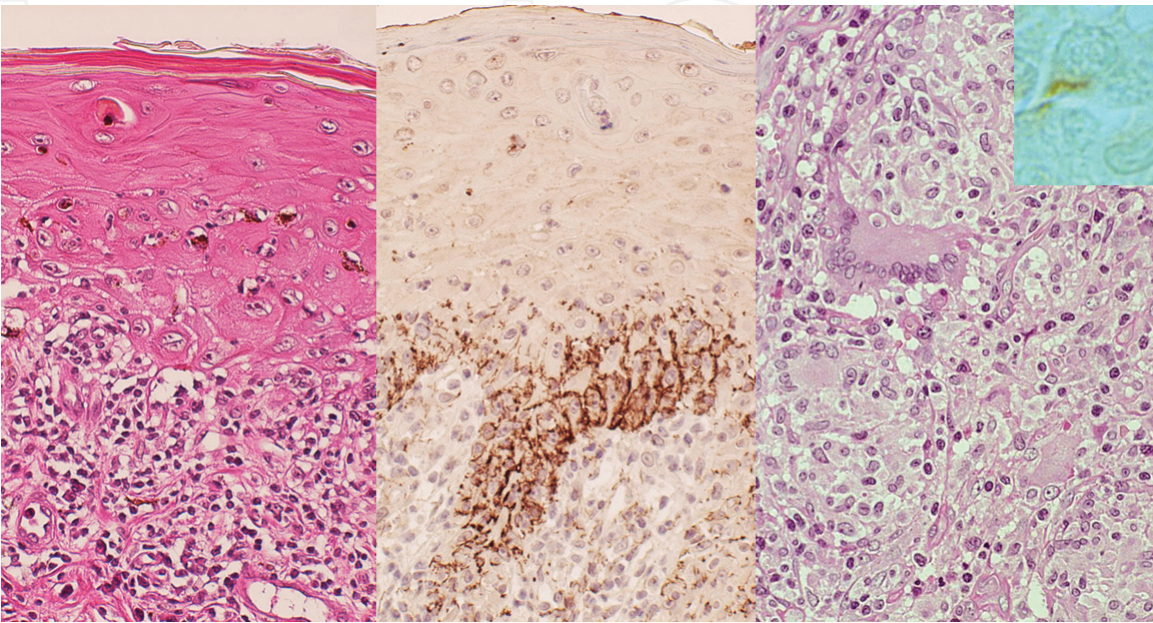
Figure 6.
T. pallidum *immunostaining II (left and center, stage I penile chancre; right, stage III syphilitic lymphadenitis; left and right, H&E; center and inset, immunostaining using* T. pallidum *antiserum). In the penis, numerous spiral microbes are clustered mainly in the basal part of the squamous mucosa and around the dermal capillary vessels. In the stage III lesion accompanying granulomatous reaction with multinucleated giant cells, coiled spirochetes are infrequently identified (inset).*
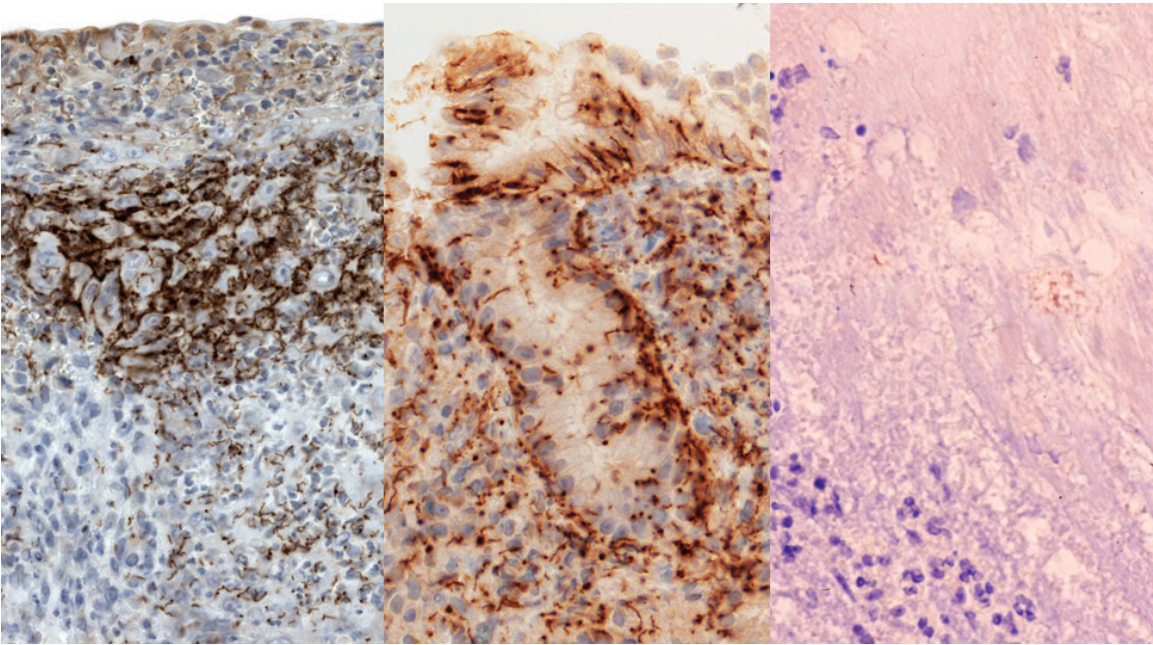
Figure 7.
T. pallidum *immunostaining III (left, tonsil; center, gastric mucosa; right, aortic valve). Immunohistochemical visualization of spirochetes in the biopsy specimens using* T. pallidum *antiserum significantly contributes to confirming the clinical and serological diagnosis of syphilis haphazardly affecting the tonsil, gastric mucosa, and aortic valve.*
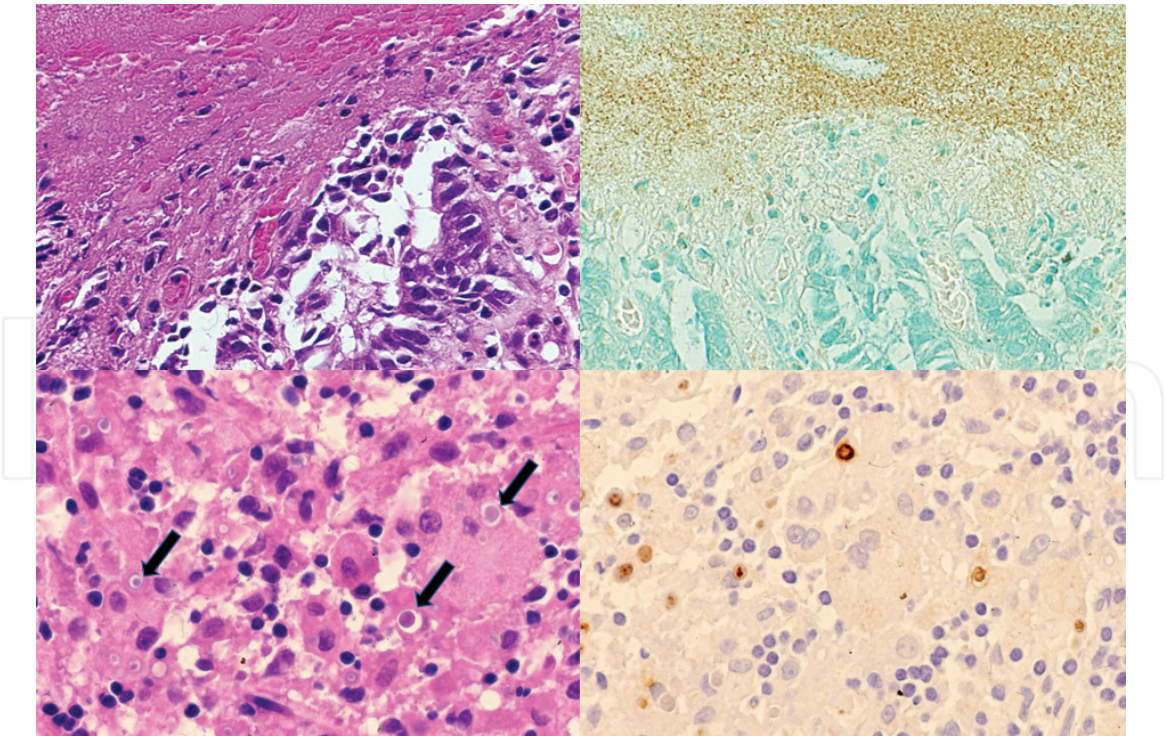
Figure 8.
E. coli *immunostaining I (upper panels, rectal erosion; lower panels, rectal malacoplakia; left, H&E; right, immunostaining using* E. coli *antiserum).* E. coli-*related antigens are detectable in eroded surface of rectal mucosa and in malacoplakia of the rectum. Michaelis-Gutmann bodies (arrows) in the cytoplasm of macrophages, the microscopic hallmark of malacoplakia, are round, basophilic, and immunoreactive to* E. coli *antigens.*
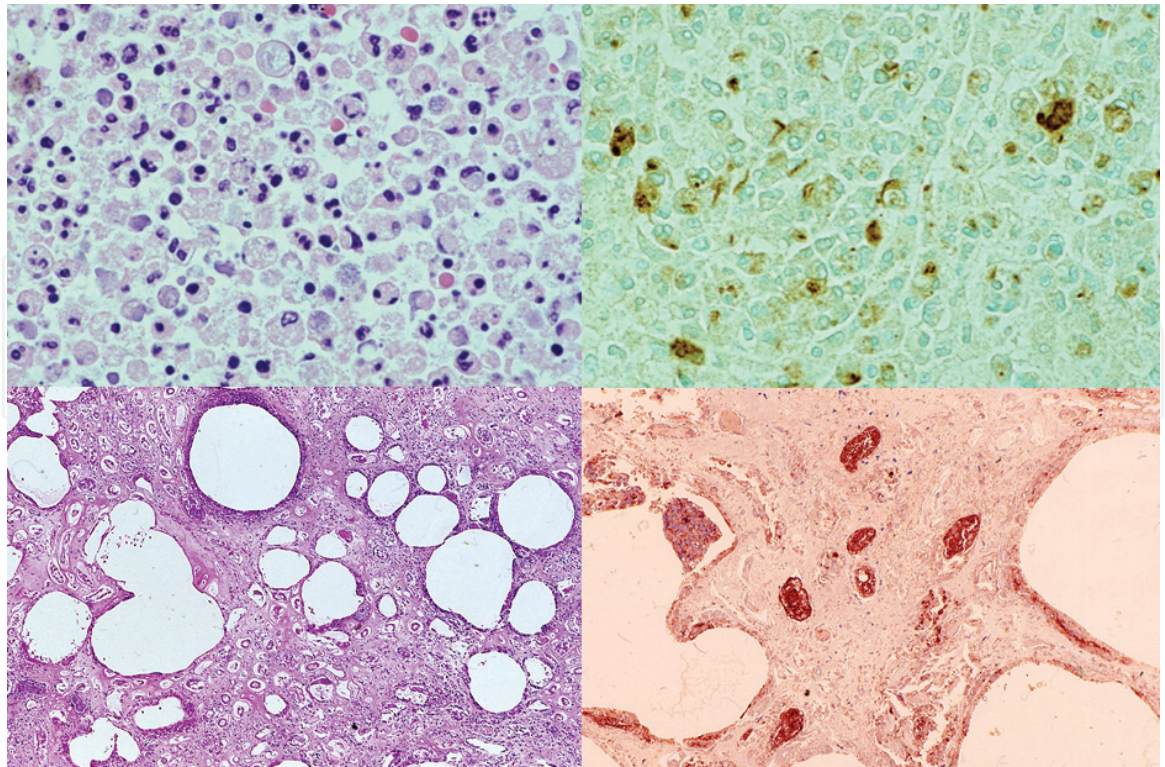

Figure 9.
E. coli *immunostaining II (upper panels, opportunistic* E. coli-*induced pneumonia; lower panels,* E. coli-*induced emphysematous pyelonephritis in a diabetic patient; left, H&E; right, immunostaining using* E. coli *antiserum). Positive rod-shaped signals are clearly seen in the cytoplasm of phagocytes in nosocomial bronchopneumonia and in severely affected kidney with numerous colonies of gas-forming bacteria.*

Immunostaining was considerably supportive and useful in the clinical practice, when treponemal microbes were visualized in the tonsillar, gastric, and aortic valvular biopsy specimens (**Figure 7**).

3.4 Immunostaining for infection of *E. coli* and related bacteria using *E. coli* antiserum

Immunostaining (Simple Stain-Max, Nichirei) using *E. coli* rabbit antiserum (Dako) diluted at 1:20,000 after proteinase K pretreatment is applicable to demonstrating infection of *E. coli* or related enterobacteria in paraffin sections. *E. coli*-related antigens were immunodetected in colonic erosion and malacoplakia in the rectal mucosa (**Figure 8**) [4, 7, 8, 10, 28]. Malacoplakia is a variant of xanthogranulomatous inflammation caused by *E. coli*, and Michaelis-Gutmann bodies, a microscopic hallmark of malacoplakia, are immunoreactive for *E. coli* antigens [28]. *E. coli*-like organisms were immunohistochemically detected in xanthogranulomatous proctitis, cholecystitis, and cholangitis, as well as abscess-forming epididymitis [4, 29, 30]. Positive granular signals in *E. coli*-induced bronchopneumonia [31] and emphysematous pyelonephritis are illustrated in **Figure 9**.

4. Immunohistochemical demonstration of bacterial antigens using four kinds of antibacterial antisera with a wide cross-reactivity to a variety of bacteria

We diagnostic pathologists encounter lesions strongly suggestive of infection but with poor clinical information or with difficulty in microscopically supposing a causative pathogen. In such situations, immunostaining employing the abovementioned four kinds of rabbit antisera is worthy of application [8, 19]. We can prove the existence of pathogens in a certain part of the lesion. Background staining is negligible, whereas *B. cereus* antiserum may be cross-reactive to the nuclei of human cells in some cases (see **Figure 16**). In this type of application, we must abandon the specificity of immunostaining, and instead we welcome to accept the sensitivity of detection.

Regrettably enough, the availability of antisera against microbes from commercial sources has become limited. In fact, antisera against BCG and *E. coli* are no longer available from Dako (Agilent) company [16]. The author is afraid that this may hamper the standardization of immunohistochemical diagnosis of infectious diseases.

Table 3 summarizes reactivities of various microbes to the four kinds of rabbit antibacterial antisera.

4.1 *E. coli* antigens in leptospirosis

Hamster liver experimentally infected with *Leptospira interrogans* is shown in **Figure 10**. Not only *Leptospira* antiserum (the gift from Prof. Shinichi Yoshida, Department of Bacteriology, Faculty of Medical Sciences, Kyushu University, Fukuoka) but also *E. coli* antiserum were reactive to spiral-shaped bacteria in the hepatic sinusoid [19]. Pathogens phagocytized by activated Kupffer cells were visualized only by *Leptospira* antiserum [32]. *E. coli* antiserum was not cross-reactive with *T. pallidum* in the syphilitic lesion, while *T. pallidum* antiserum was unreactive with *Leptospira* in the hamster liver.

Bacterium	Anti-*B. cereus*	Anti-BCG	Anti-*T. pallidum*	Anti-*E. coli*
Leptospira interrogans	ND	−	−	+
Serratia marcescens	ND	−	+	+
Brachyspira sp.	+	+	+	+
Non-tuberculous *Mycobacterium*	ND	+	+	−
Vibrio vulnificus	+	+	+	+
Bordetella pertussis	+	+	+	−
Haemophilus influenzae	+	+	+	−
Actinomyces israelii	+	+	+	−
Nocardia beijingensis	+	+	+	−
Bartonella henselae	ND	+	+	−
Corynebacterium kroppenstedtii	+	+	+	(+)
Klebsiella rhinoscleromatis	+	(+)	−	−
Propionibacterium acnes	+	−	−	−
Pseudomonas aeruginosa	+	−	−	−
Gram-positive cocci causing				
Brain abscess	+	−	−	−
Chorioamnionitis	+	−	−	−

ND, not done, (+), focally positive.
Reactivities of various pathogens to commercial rabbit antisera against B. cereus, *BCG,* T. pallidum, *and* E. coli *are summarized.*

Table 3.
Reactivities of various microbes to the four kinds of rabbit antibacterial antisera.
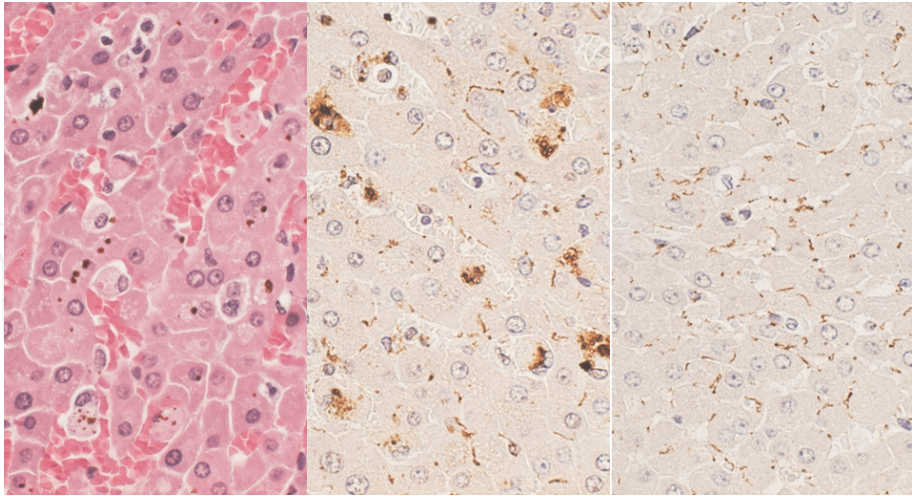
Figure 10.
Hamster liver in experimental leptospirosis (left, H&E; center, Leptospira *antigens; right,* E. coli *antigens). Liver cell cords are disarranged due to infection of* Leptospira interrogans. *Not only* Leptospira *antiserum but also* E. coli *antiserum decorate spiral-shaped bacteria in the sinusoid. Pathogens phagocytized by activated Kupffer cells are visualized only by* Leptospira *antiserum.*

4.2 Application to *Serratia* septicemia

Serratia marcescens, a red colony-forming Gram-negative rod usually showing low virulence, may cause opportunistic infection in immunosuppressed
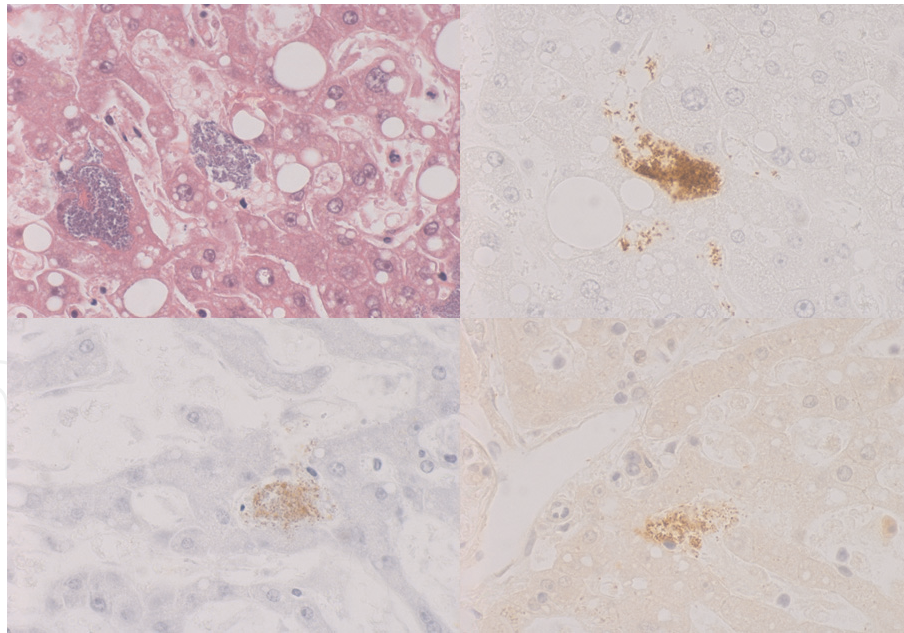
Figure 11.
Serratia marcescens *septicemia forming colonies in the sinusoid of autopsied liver (left upper, H&E; right upper,* E. coli *LPS; left lower,* E. coli *antigens; right lower,* T. pallidum *antigens). Colonies of Gram-negative microbes reveal positivity for both* E. coli *antigens and* T. pallidum *antigens, in addition to strong reactivity to monoclonal antibody 2D7/1 against* E. coli *LPS.*

patients [33]. **Figure 11** illustrates the autopsied liver of a Japanese female aged 70's complicated by *S. marcescens* septicemia. Colonies of Gram-negative microbes were observed in the sinusoid of the liver. Comparative immunostaining disclosed positivity for both *E. coli* antigens and *T. pallidum* antigens, in addition to strong reactivity to monoclonal antibody 2D7/1 against *E. coli* LPS (Abcam) [19].

4.3 Application to intestinal spirochetosis

Intestinal spirochetosis is caused by localized infection of *Brachyspira aalborgi* or *B. pilosicoli* on the colonic mucosa. Basophilic brush border-like structures are recognized in H&E-stained sections [34]. It has been clarified that the brush border-like structures by zoonotic *B. pilosicoli* are much longer than those by *B. aalborgi* [35]. The surface-adherent bacteria were clearly visualized by immunostaining with *T. pallidum* monoclonal antibody (J010J), and the spirochete was also proven by immunostaining with antisera against *T. pallidum*, BCG, *E. coli*, and *B. cereus*, as shown in **Figure 12** [13, 19]. Antisera against *Leptospira* and *Helicobacter pylori* also cross-reacted to the pathogen.

4.4 Cross-reactivity to acid-fast bacilli

Non-tuberculous mycobacteria (*Mycobacterium avium-intracellulare*) in a caseous necrotic lesion of the lung were demonstrated not only by BCG antiserum but also by *T. pallidum* antiserum, as illustrated in **Figure 13** [19]. BCG antiserum was also strongly reactive with amorphous background substances, probably representing decayed bacterial proteins.

4.5 Application to *Vibrio vulnificus* infection

Gangrenous lesions in the extremity caused by lethal *Vibrio vulnificus* infection (flesh-eating disease) microscopically show active growth of Gram-negative
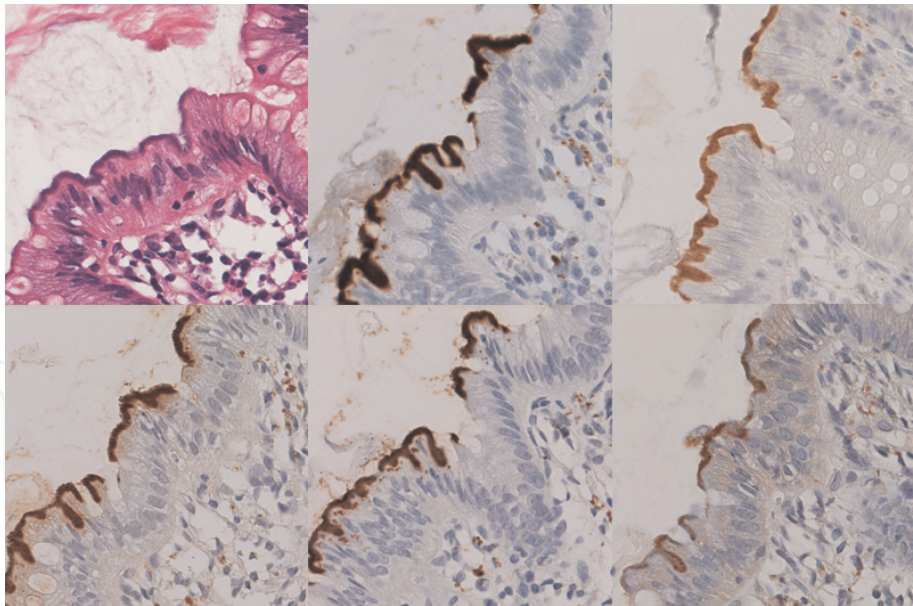
Figure 12.
Intestinal spirochetosis (left upper, H&E; center upper, reactivity with T. pallidum *monoclonal antibody J010J; right upper, reactivity with* T. pallidum *antiserum; left lower, BCG antigens; center lower,* E. coli *antigens; right lower, Leptospira antigens). The colonic mucosal surface-adherent, brush border-like basophilic bacteria (*Brachyspira aalborgi*) are visualized by monoclonal and polyclonal antibodies to* T. pallidum*, as well as by immunostaining with antisera to BCG,* E. coli, *and* Leptospira.
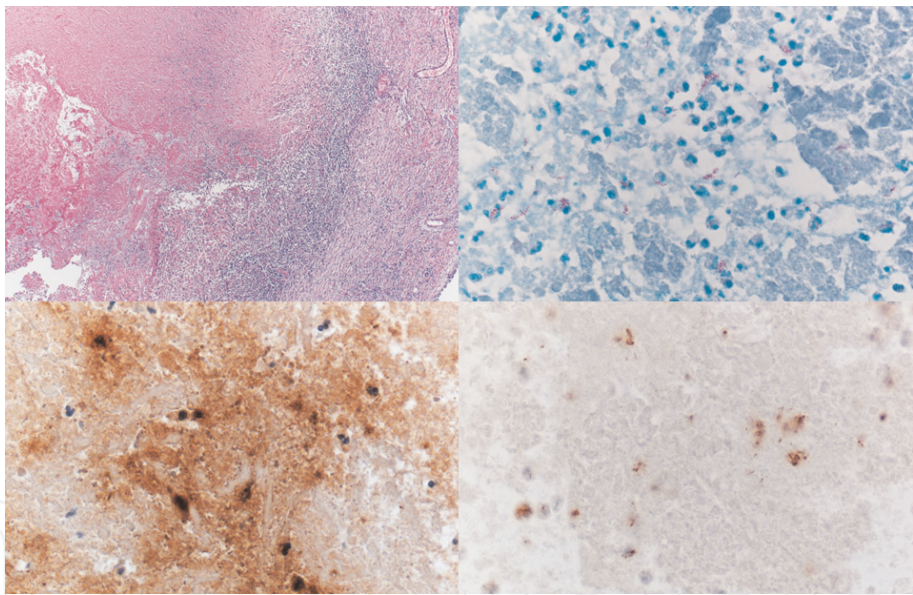
Figure 13.
Non-tuberculous mycobacteriosis of the lung caused by Mycobacterium avium-intracellulare *(left upper, H&E; right upper, acid-fast stain; left lower, BCG antigens; right lower,* T. pallidum *antigens). Acid-fast bacilli seen in caseous necrosis are labeled with both antisera. BCG antiserum also strongly reacts with background degradative substances.*

bacteria in soft tissue [36]. The bacteria were immunolocalized with antisera against BCG, *B. cereus*, and *T. pallidum* (**Figure 14**) [8, 19]. *E. coli* antiserum was scarcely reactive.

4.6 Application to pertussis

Bordetella pertussis infection (pertussis) may cause severe illness leading the child to death [37]. The lung shows microscopic features of "atypical" pneumonia. The Gram-negative bacteria phagocytized by macrophages in alveoli of the autopsied
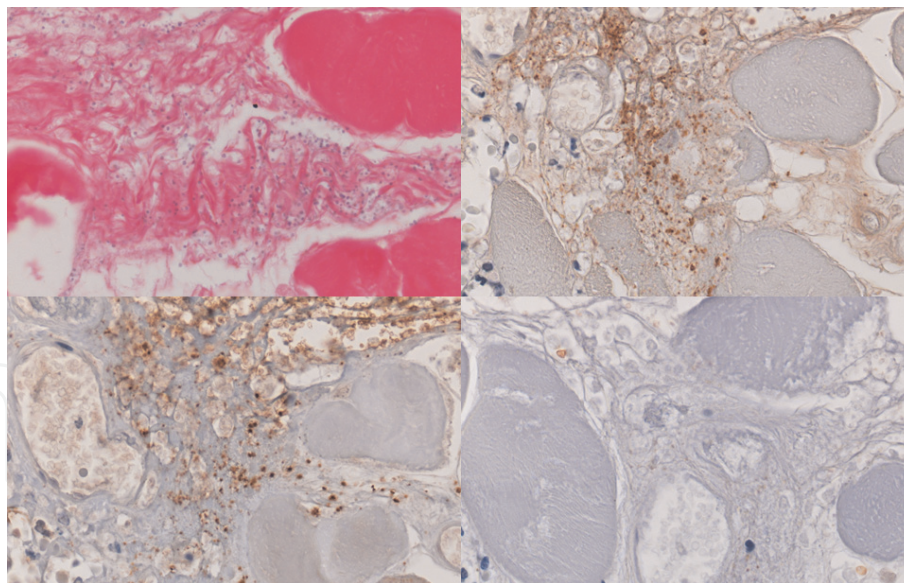
Figure 14.
Gangrene of the extremity caused by Vibrio vulnificus *infection (left upper, H&E; right upper, BCG antigens; left lower,* T. pallidum *antigens; right lower,* E. coli *antigens). Gram-negative bacteria growing among necrotic striated muscle fibers in the extremity are immunolocalized with antisera against BCG and* T. pallidum. E. coli *antiserum is scarcely reactive.*
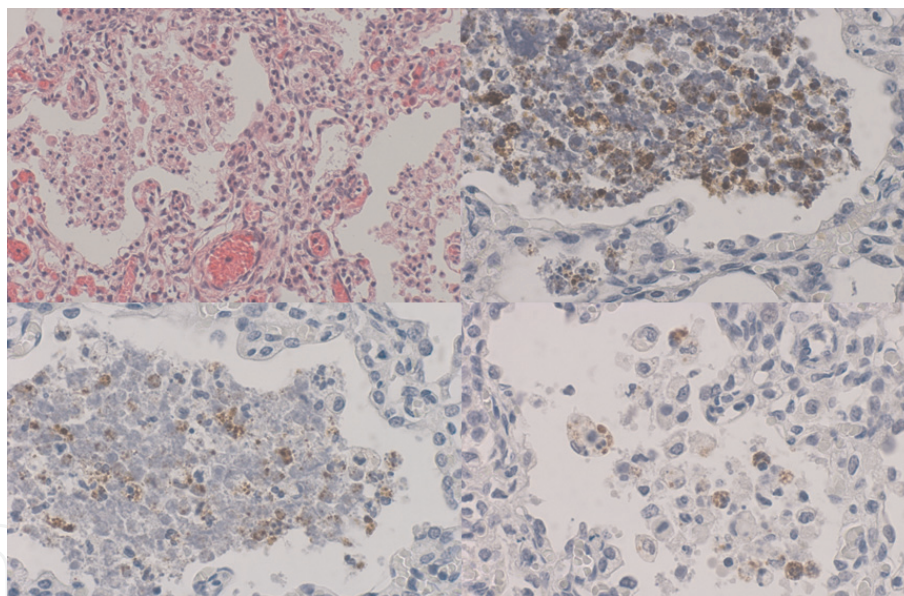

Figure 15.
Autopsied lung in pertussis (left upper, H&E; right upper, BCG antigens; left lower, B. cereus *antigens; right lower,* T. pallidum *antigens). The lung shows microscopic features of atypical pneumonia.* Bordetella pertussis *phagocytized by alveolar macrophages is demonstrable with antisera against BCG,* B. cereus, *and* T. pallidum.

lung were positively immunostained with antisera against BCG, *B. cereus*, and *T. pallidum* (**Figure 15**) [19]. *E. coli* antiserum was scarcely reactive.

4.7 Application to *Haemophilus influenzae* infection

Haemophilus influenzae may cause tonsillar ulcer in children and young adults [38]. A biopsy material from the ulcerated tonsil of a young male revealed dense infection of Gram-negative rods on the ulcer base. Antisera against BCG, *B. cereus*, and *T. pallidum* demonstrated the pathogen (**Figure 16**) [19]. Again, *E. coli* antiserum was scarcely reactive.

4.8 Application to actinomycosis

Secondary dense infection of *Actinomyces israelii* is occasionally observed in biopsied sequestrum of the alveolar bone of the jaw [39]. Grocott-positive filamentous bacteria occupy the marrow space but with little inflammatory reaction. The microbes were visualized not only with *A. israelii* monoclonal antibody (396AN1) but also with antisera against BCG and *B. cereus* (**Figure 17**) [19]. Reactivity with antisera against *T. pallidum* and *E. coli* was faint.

4.9 Application to nocardiosis

Nocardiosis is caused by filamentous Gram-positive saprophytic bacteria, *Nocardia* spp., mainly in the lung. This weakly acid-fast aerobe infects mainly in the immunocompromised patients. *N. asteroides* is the most frequent isolate, but other species may also be encountered [40]. A subpleural nodule in the left upper lobe
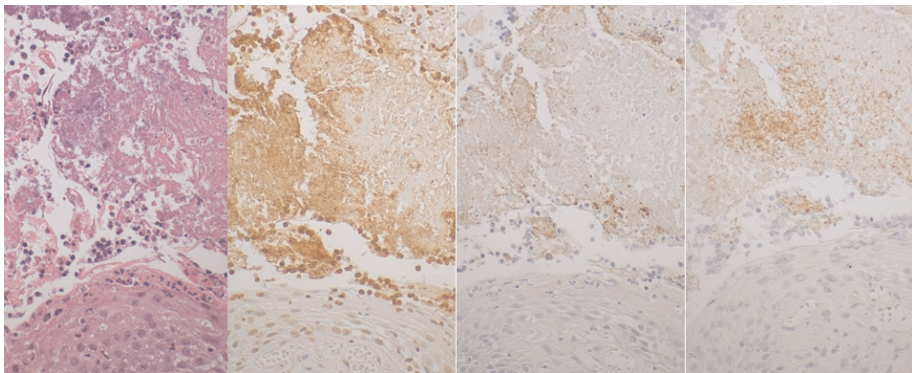
Figure 16.
Haemophilus influenzae-*induced tonsillitis (left, H&E; center left,* B. cereus *antigens; center right, BCG antigens; right,* T. pallidum *antigens). Antisera against* B. cereus, *BCG, and* T. pallidum *demonstrate* H. influenzae *colonizing the tonsillar ulcer.* B. cereus *antigens are expressed with the strongest reactivity, while cross-reactivity to the nucleus of human cells is seen.*
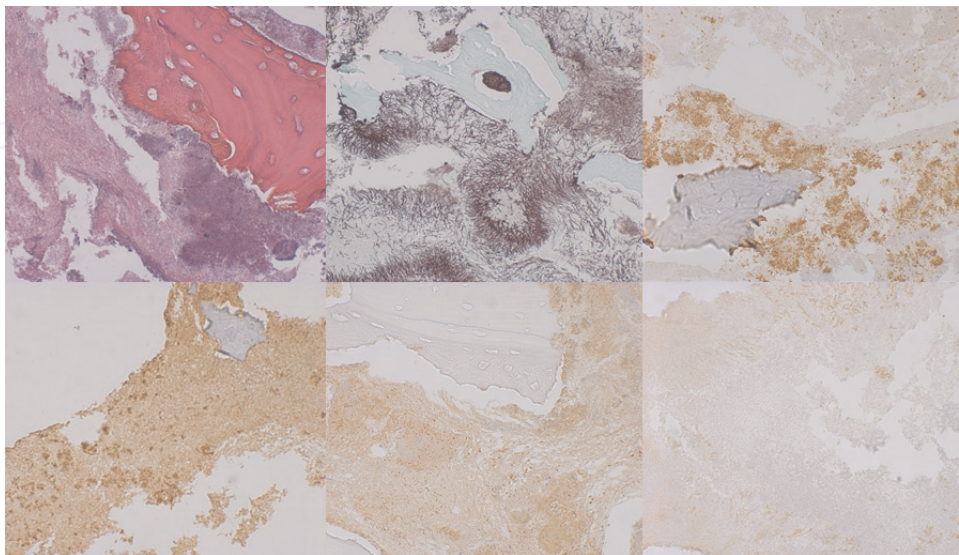

Figure 17.
Actinomyces israelii *colonizing the sequestration of the jaw bone (left upper, H&E; center upper, Grocott stain; right upper, reactivity with* A. israelii *monoclonal antibody 396AN1; left lower,* B. cereus *antigens; center lower, BCG antigens; right lower,* T. pallidum *antigens). The marrow space among dead bone trabeculae is occupied by Grocott-positive filamentous bacteria but with little inflammatory reaction. The pathogen is immunolocalized not only by the monoclonal Antibody but also by antisera against* B. cereus *and BCG.* T. pallidum *antigens are scarcely expressed.*
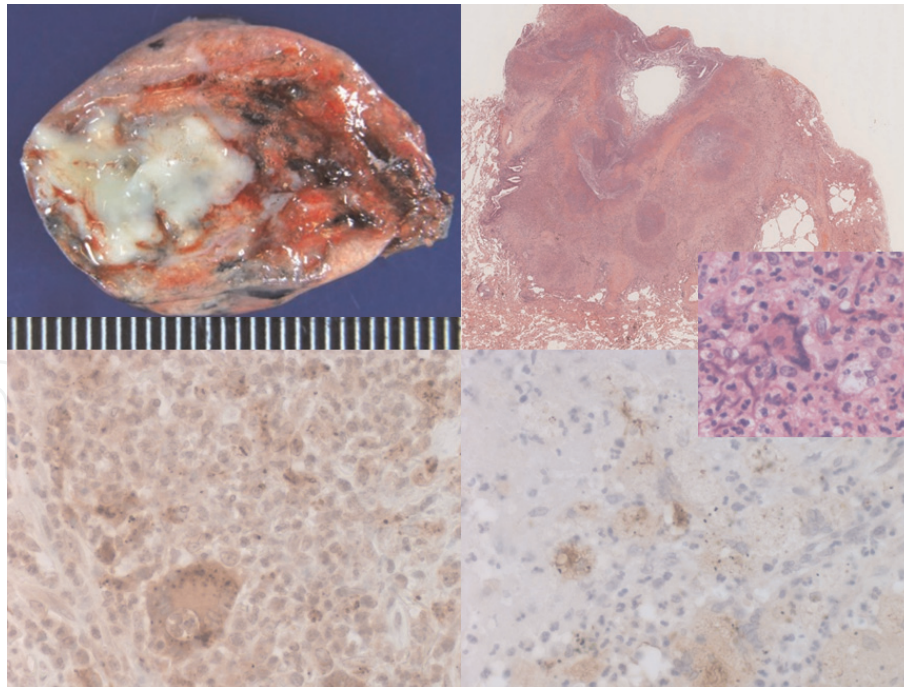
Figure 18.
Pulmonary nocardiosis caused by Nocardia beijingensis *(left upper, gross picture; right upper, low-powered H&E; inset, high-powered H&E; left lower,* B. cereus *antigens; right lower, BCG antigens). Subpleural abscess seen in a diabetic aged with steroid therapy was surgically excised. Necrotic lesions reveal focal clusters of foamy macrophages and a few multinucleated giant cells. Grocott stain failed to identify the pathogen. Antisera against* B. cereus *and BCG clearly demonstrate filamentous and aggregated microbes in the cytoplasm of foamy macrophages and giant cells.*

was pointed out in a diabetic Japanese male aged 70's who also suffered from nephrotic syndrome with steroid administration. Video-assisted thoracic surgery disclosed necrotic nodule grossly resembling a tuberculous lesion. Microscopically, abscess formation with foamy cells clustering and occasional multinucleated giant cell reaction was confirmed, and *N. beijingensis* was isolated and molecularly confirmed by analyzing 16S ribosomal RNA. Grocott, periodic acid-Schiff, Gram, and Ziehl-Neelsen stains were all negative. Immunostaining using antisera against *B. cereus* and BCG clearly demonstrated filamentous or aggregated bacteria phagocytized by foamy cells and multinucleated giant cells (**Figure 18**). Some bacteria reacted to *T. pallidum* antiserum, while *E. coli* antiserum was unreactive.

4.10 Application to bartonellosis

Cervical lymphadenopathy in cat-scratch disease, infection of *Bartonella henselae*, is microscopically characterized by suppurative granuloma formation. Not only cat scratch but also bite by cat flea can provoke bartonellosis [41]. Splenic abscess is occasionally seen as systemic manifestation of cat-scratch disease [42]. Splenectomy was performed from a male patient aged 40's. Monoclonal antibody H2A10 to *B. henselae* (not cross-reactive to non-henselae *Bartonella*) [41] demonstrated a few microbes in the cytoplasm of macrophages accumulated in the abscess cavity. The positive findings were more easily obtained by immunostaining with antisera against BCG and *T. pallidum* (**Figure 19**) [19].

4.11 Application to granulomatous mastitis

Granulomatous mastitis is seen in childbearing women 2–4 years after breastfeeding [43]. The causative agent is lipophilic Gram-positive bacillus,

Corynebacterium kroppenstedtii, and the lesion is microscopically featured by lipid droplet-centered abscess or epithelioid granuloma. Antisera against BCG, *B. cereus*, and *T. pallidum* demonstrated bacterial cross-reactive antigens mainly in the lipid droplet surrounded by abscess and/or granuloma (**Figure 20**) [8, 16, 19]. The antigens were occasionally seen in the cytoplasm of macrophages clustered in the inflammatory lesion. *E. coli* antigens were infrequently seen in the lesion.
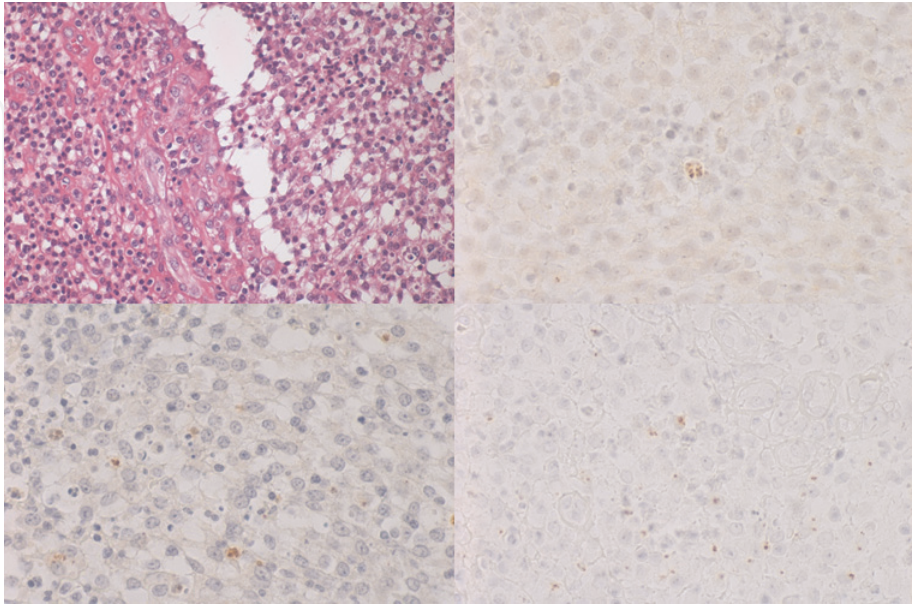

Figure 19.
Splenic bartonellosis (left upper, H&E; right upper, reactivity with Bartonella henselae *monoclonal antibody H2A10; left lower, BCG antigens; right lower,* T. pallidum *antigens). Suppurative granulomas are formed in the spleen. Macrophages in the abscess cavity focally reveal dot-like positive signals not only by the monoclonal antibody but also by antisera against BCG and* T. pallidum. *Of note is that more signals are seen with the two antisera than with the monoclonal antibody.*
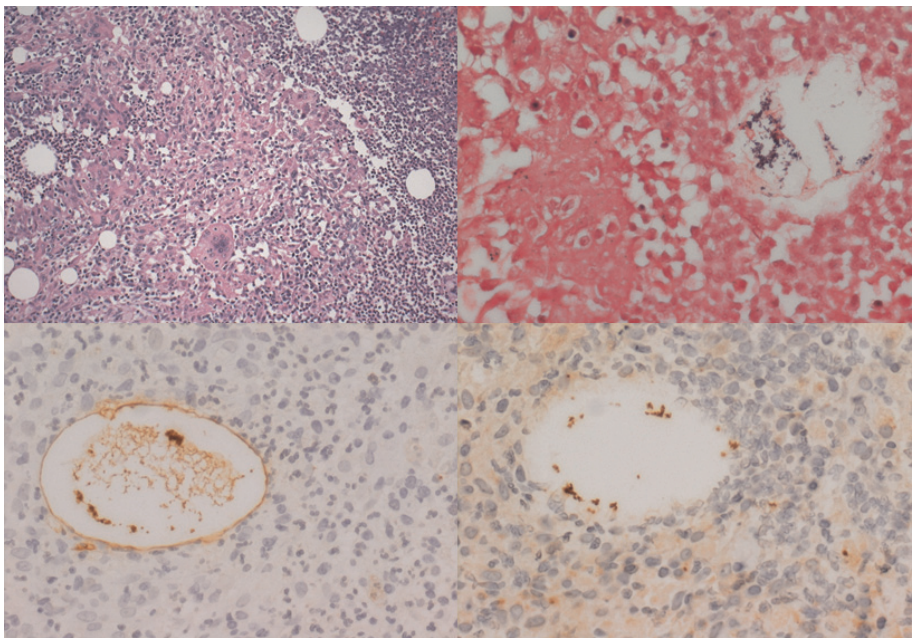

Figure 20.
Granulomatous mastitis caused by Corynebacterium kroppenstedtii *(left upper, H&E; right upper, Gram stain; left lower, BCG antigens; right lower,* T. pallidum *antigens). This lactation-related infection is microscopically featured by lipid droplet-centered abscess or epithelioid granuloma. Gram stain and immunostaining for* BCG, B. cereus, *and* T. pallidum *demonstrate bacterial colonies in the lipid droplet surrounded by inflammatory reactions.*

It should be of note that the positive signals were identified at the site of the disease-specific lesion. Polymerase chain reaction (PCR) analysis using DNA extracted from paraffin sections confirmed the nucleotide sequence of *C. kroppenstedtii* [16].

4.12 Application to rhinoscleroma

Rhinoscleroma is localized and indolent infective nodule in the nasal cavity, endemic in Egypt, South America and eastern Europe. The main causative microbe has been reported to be *Klebsiella rhinoscleromatis*. Microscopically, foamy macrophages phagocytizing gram-negative rods, so-called Mickulicz cells, are observed in chronic inflammatory infiltrates [44]. A Japanese male aged 70's complained of a single elevated nodule in the nasal vestibule. Biopsy revealed localized infiltration of foamy macrophages in the background of chronic inflammation. Round vacuoles with short rod-like material were occasionally seen in the macrophages or Mickulicz cells [45]. Immunostaining disclosed positive findings with monoclonal antibody 70-2 against *Klebsiella* spp., and the antiserum against *B. cereus* gave similar positivity. Fewer cells were also reactive to BCG antiserum. Antisera against *T. pallidum* and *E. coli* failed to detect the intracellular microbes (**Figure 21**). Negativity to *E. coli* antiserum was an unexpected finding, because of the close relationship between the two enterobacteria.

4.13 Immunostaining with *B. cereus* antiserum showing the widest cross-reactivity among four

In certain lesions, *B. cereus* antiserum was reactive to the pathogen, while the other three antisera were poorly reactive. It is plausible that antiserum against *B. cereus*, a Gram-positive spore-forming rod, shows the widest cross-reactivity including Gram-positive bacteria. Bacterial microbes positive for *B. cereus*-related antigens were demonstrated in brain abscess, placental chorioamnionitis, and *Propionibacterium acnes*-induced folliculitis of the skin (**Figure 22**) (refer also to **Figure 45** for *P. acnes* folliculitis). Positive signals of *B. cereus* antigens in a lethal adult case of *Pseudomonas aeruginosa*-induced pneumonia/septicemia are demonstrated in **Figure 23** [19].
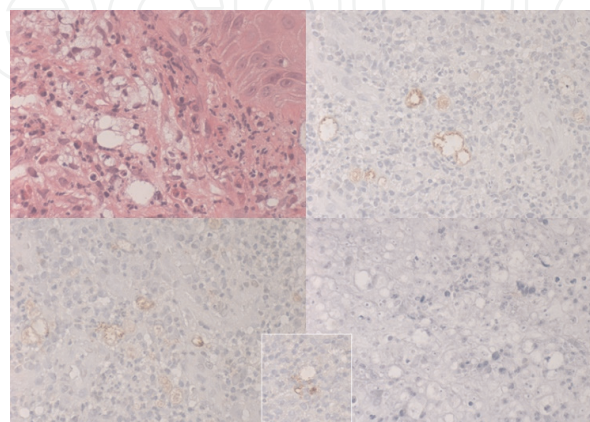

Figure 21.
Rhinoscleroma caused by Klebsiella rhinoscleromatis (left upper: H&E, right upper: reactivity with monoclonal antibody 70-2 to Klebsiella spp., left lower: B. cereus antigens, right lower: E. coli *antigens, inset: BCG antigens). Foamy macrophages with intracytoplasmic vacuoles containing short rod-like material (Mickulicz cells) are immunoreactive with monoclonal antibody 70-2 to* Klebsiella *spp. and* B. cereus *antiserum. Fewer cells are labeled with BCG antiserum, while* E. coli *antiserum is unreactive.*
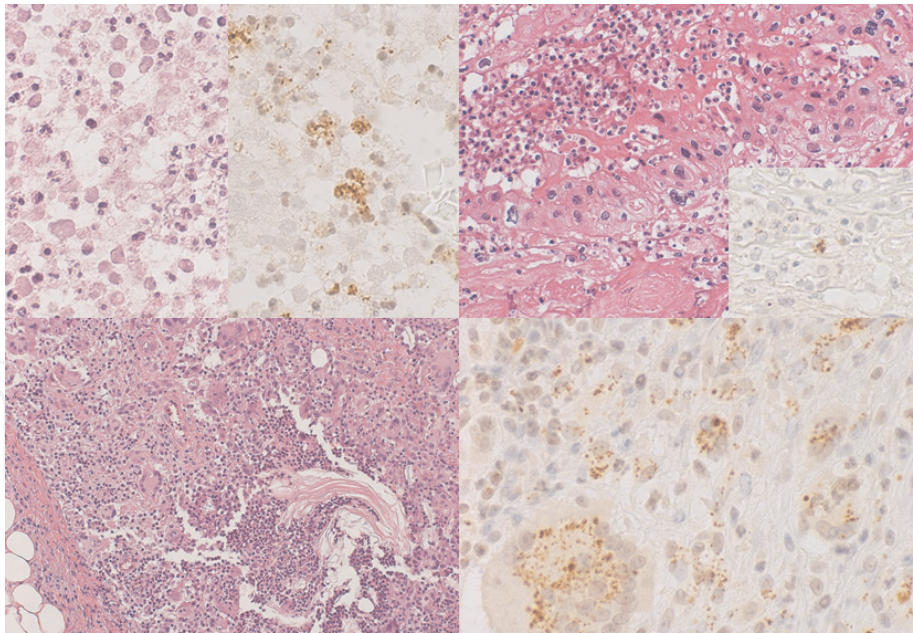
Figure 22.
The widest cross-reactivity shown by Bacillus cereus antiserum (left upper, brain abscess; right upper, ascending chorioamnionitis of placenta; lower panels, Propionibacterium acnes-induced folliculitis of the chest, combination of H&E, and B. cereus *immunostaining). Gram-positive bacterial microbes are visualized by immunostaining with* B. cereus *antiserum. No positivity is seen with BCG,* T. pallidum*, and* E. coli *antisera.*
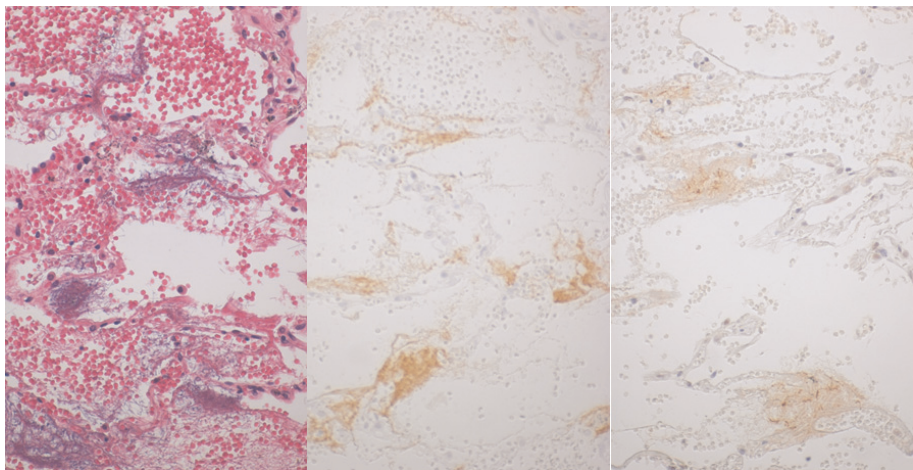

Figure 23.
Lethal Pseudomonas aeruginosa *pneumonia/septicemia (left, H&E; center, immunostaining using monoclonal antibody B11; right, immunostaining using* B. cereus *antiserum). Gram-negative bacilli grow along the alveolar septum, and no cellular reactions are noted. Immunoreactive signals are observed with the monoclonal antibody, as well as with* B. cereus *antiserum.*

5. Use of patients' sera for demonstrating the target pathogens in paraffin sections

Sera of patients suffering from infectious diseases expectedly contain high-titer IgG-type antibodies against the causative microbe, particularly when inflammatory reactions such as abscess and granuloma are histopathologically confirmed in immunocompetent individuals. It is well known that 2 weeks is needed to have specific antibodies to be raised in the serum. The diluted patients' serum can be used as a probe for indirect immunoperoxidase staining on histopathologic specimens routinely embedded in paraffin [4, 7, 8, 20–23]. A variety of infectious microbes were demonstrable with reliable sensitivity but limited specificity, as indicated below. Endogenous human immunoglobulins (IgG) in formalin-fixed,

paraffin-embedded sections were scarcely detected by the peroxidase-labeled secondary antihuman immunoglobulins. High-sensitivity detection sequence such as the labeled polymer method naturally leads to high-background staining, because of the detection of endogenous immunoglobulins in sections. The method is simple, economic, useful, and beautiful for the histopathologic diagnosis of infectious diseases, and it is particularly suitable for the developing countries, since the patient's serum is free in charge. This approach is especially effective for detecting protozoa and helminth [22], because the specific antibodies are often commercially unavailable.

There are two situations. In some cases, the causative pathogen has been identified by clinical, laboratory, and/or histopathological analysis, and thus the specificity of the patient's serum can be expected before immunostaining. In other cases, the causative pathogen is unsettled yet or unknown. In the latter situation, the patient's serum functions as a low-specificity and high-sensitivity probe in immunostaining.

Table 4 summarizes patients' sera applicable to immunostaining in paraffin sections.

5.1 Methodology

Human tissues and organs, obtained either by biopsy, during surgery or at autopsy, were routinely fixed in 10% unbuffered or buffered formalin for 1 day to 4 weeks. The indirect immunoperoxidase technique was applied to deparaffinized sections [4, 7, 8, 20–23]. The serum of patient, principally not in an immunocompromised state, was diluted at 1:500 or 1:1000 and was incubated for 30 min or overnight. In case of protozoan infection, the presence of high-titer IgG antibodies in the patients' serum was commonly confirmed by immunofluorescence titration, as shown in **Table 4**. The serum from patients positive for human immunodeficiency virus (HIV) or hepatitis virus markers must not be utilized, in order to avoid biohazard. The serum of immunocompromised, non-HIV patients may be utilized after dilution at 1:5 or 1:10. The second layer reagent was horseradish peroxidase-labeled goat IgG to human immunoglobulins (Dako/Agilent) at a 1:50 dilution. Endogenous peroxidase activity was quenched in methanol containing 0.3% hydrogen peroxide for 20 min. No other pretreatment procedures such as proteinase digestion or heat-induced antigen retrieval were needed, but heating pretreatment was infrequently necessary for certain instances (e.g., the detection of free-living amoeba, *Balamuthia*; see below). Therefore, the author recommends introducing a heat-induced antigen retrieval procedure in 10 mM citrate buffer, pH 6, for immunostaining using silane (3-aminopropyltrimethoxysilane)-coated glass slides. After the diaminobenzidine coloring reaction, the nuclei were counterstained with 5% methyl green or Mayer's hematoxylin. When necessary, paraffin sections of related or unrelated infectious lesions were immunostained to confirm the cross-reactivity or specificity of the patients' serum.

It is of notice that IgG in the patients' serum may show cross-reactivity to related pathogens to certain or considerable degrees [4, 20, 21]. In bacterial and fungal infections, the sera often serve as pan-bacterial or pan-fungal probes. The cross-reactivity may result from the naturally acquired antibodies in healthy individuals [20]. In viral, protozoan, and helminthic infections, in contrast, high-grade specificity with limited cross-reactivity can be expected [22]. When the specificity of the sera of patients with parasitic infestation is known, it is sufficiently satisfactory to enable them to be employed as specific antibody reagents for the following new cases.

5.2 Immunostaining using sera of patients with established diagnosis

Here, the immunohistochemical application of sera of patients with established or fixed diagnosis is shown, including bacterial, fungal, viral, protozoan, and helminthic infections.

Infectious disease	Serum dilution	Comments
Tsutsugamushi disease (scrub typhus)	1:100	Immunoelectron microscopy performed
Staphylococcal pyoderma	1: 500	*Staphylococcus aureus* cultured
Propionibacterium acnes folliculitis	1:500	*P. acnes*-specific antigen PAC3 identified
Cutaneous sporotrichosis	1:500	Sporotrichin reaction positive
Malassezia (*Pityrosporum*) folliculitis	1:500	Multiple skin papules on the chest
Cutaneous alternariosis	1:500	Long-lasting skin lesion on the knee
Cutaneous cryptococcosis in leukemia	1:10	Chemotherapy with steroid administration
Hemorrhagic varicella	1:500[*]	Bone marrow transplanted acute leukemia
Cutaneous leishmaniasis (African type)	1:1000	High immunofluorescence titer
Cutaneous leishmaniasis (Indian type)	1:1000	High immunofluorescence titer
Visceral leishmaniasis (liver biopsy)	1:500	High immunofluorescence titer
Acanthamebic encephalitis	1:500	Opportunistic infection in liver cirrhosis
Amebic dysentery	1:500[*]	High immunofluorescent titer
Balamuthia encephalitis	1:500	*Balamuthia* DNA identified by PCR
Cerebral toxoplasmosis	1:1000[*]	High immunofluorescence titer
Cryptosporidiosis in AIDS	1:1000[*]	High immunofluorescence titer
Duodenal cystoisosporiasis	1:500	Chronic intractable diarrhea
Blastocystosis (cell block of cultured microbes)	1:500[*]	High immunofluorescence titer
Cutaneous gnathostomiasis	1:500	Creeping disease on the abdominal skin
Extra-gastrointestinal (omental) anisakiasis	1:500	Positive with monoclonal antibody
Liver ascariasis (surgical material)	1:500	Ouchterlony's diffusion-in-gel test positive
Japanese schistosomiasis (colon)	1:200	Calcified ova seen (healed remote case)
Bilharziasis (colon biopsy)	1:500	Spine-forming ova seen in urine
Multilocular echinococcosis	1:200	Hepatectomy specimen in Hokkaido Island
Neurocysticercosis	1:20	Multiple brain nodules

[*]*High-titer sera were obtained from other immunocompetent patients.*

Table 4.
Patients' sera applicable to immunostaining in paraffin sections.

5.2.1 Bacterial infection

5.2.1.1 Tsutsugamushi disease (scrub typhus)

Mite-borne Tsutsugamushi disease or scrub typhus endemic in Japan is caused by *Orientia tsutsugamushi* belonging to the family *Rickettsiaceae* [46]. Biopsy was performed from the mite-bite eschar, and hemophagocytic macrophages were clustered at the base of the ulcer. The diluted patient's serum gave positive granulated signals in the cytoplasm of the macrophages [23], and pre-embedding
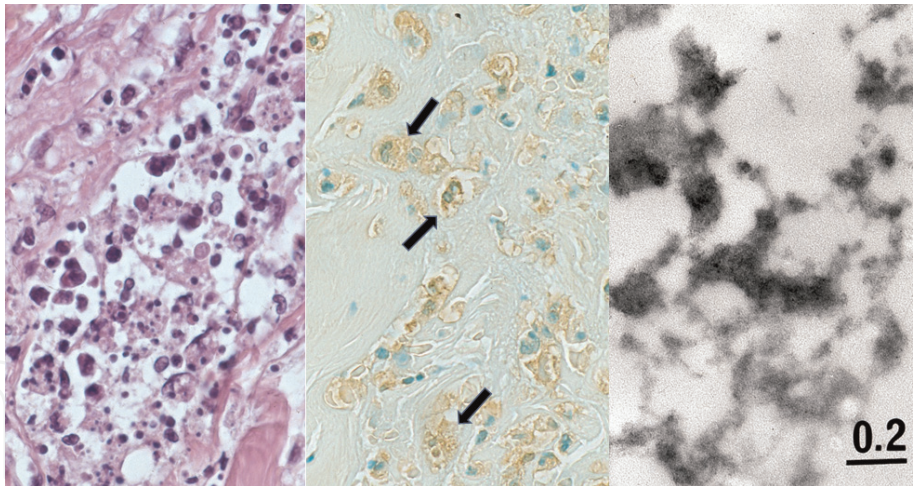
Figure 24.
Mite-bite eschar in Tsutsugamushi disease or scrub typhus (left, H&E; center, reactivity with patient's own serum; right, pre-embedding immunoelectron microscopy using paraffin section). Hemophagocytic macrophages are clustered at the base of eschar. The patient's serum gave positive granulated signals in the cytoplasm of the macrophages (arrows), and pre-embedding immunoelectron microscopy disclosed densely labeled granular material measuring 2 μm.

immunoelectron microscopy employing a paraffin section disclosed labeled granular material measuring 2 μm (**Figure 24**) [47].

5.2.1.2 Staphylococcal pyoderma

Skin biopsy specimen from *Staphylococcus aureus*-induced pyoderma reveals diffuse dermal infiltration of neutrophils and macrophages. The patient's own serum detected coccoid bacteria phagocytized by the inflammatory cells (**Figure 25**) [20, 21, 23].
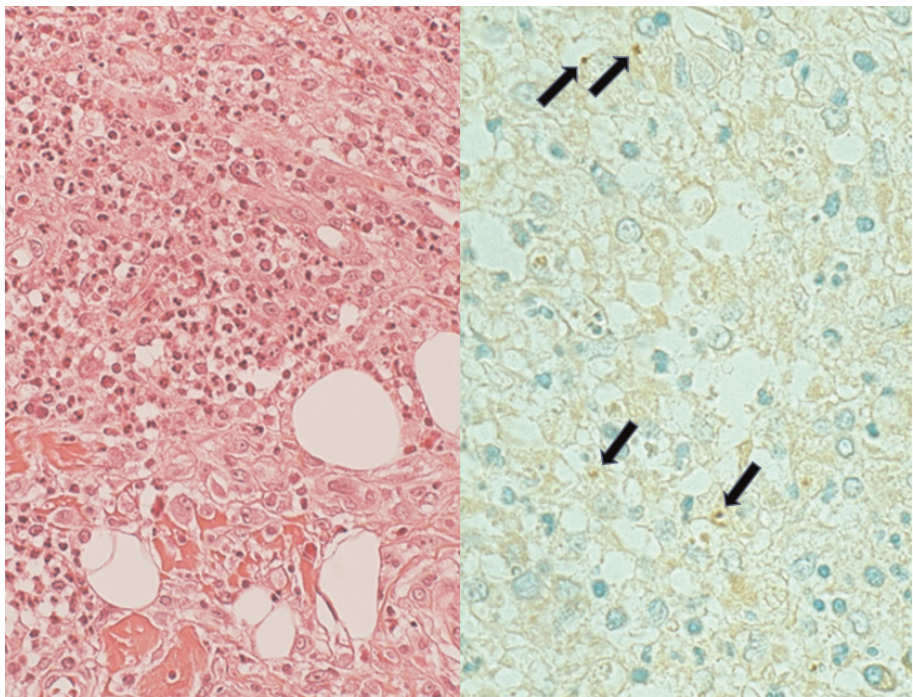
Figure 25.
Staphylococcus aureus-induced pyoderma (left, H&E; right, reactivity with patient's own serum). The dermis reveals diffuse infiltration of neutrophils and macrophages. The patient's own serum detects coccoid bacteria phagocytized by the inflammatory cells (arrows).

5.2.2 Fungal infection

5.2.2.1 Sporotrichosis

Sporotrichosis, skin infection of a dimorphic fungus *Sporothrix schenckii* particularly endemic in tropical and subtropical areas, is mediated by traumatic inoculation from soil or plants [48]. Skin biopsy material of sporotrichosis shows suppurative granuloma formation in the dermis. Periodic acid-Schiff-reactive small yeast-like fungal cells phagocytized by macrophages or multinucleated giant cells were reactive with the patient's own serum (**Figure 26**) [20, 21, 23].

5.2.2.2 Malassezia *folliculitis*

Malassezia (*Pityrosporum*) folliculitis commonly seen on the face and upper portion of the trunk has been confused with acne vulgaris [49]. A dilated hair follicle in the biopsy material was infiltrated by neutrophils and epithelioid cells forming suppurative granuloma. The patient's own serum reacted to Grocott-positive yeast-like fungi in the lesion (**Figure 27**) [21, 23]. Malassezial bodies, a commensal in the hair follicle of normal seborrheic skin sampled from another patient, were strongly labeled with the same serum.

5.2.2.3 Cutaneous alternariosis

Alternaria is a nonpathogenic, melanin-forming fungus widely seen in the environment. Rarely, skin infection of *A. alternata* happens [50]. In a skin biopsy specimen from a young female, a few Grocott-reactive fungi were observed in the chronically inflamed dermis. The patient's own serum visualized the fungal microbes phagocytized by macrophages (**Figure 28**) [21, 23].

5.2.2.4 Cryptococcosis complicated in an immunocompromised state

Cutaneous lesions occur in 10-20% of life-threatening disseminated cryptococcosis seen in immunocompromised patients [51]. Opportunistic skin infection of *Cryptococcus neoformans* occurred in a young patient after chemotherapy and steroid
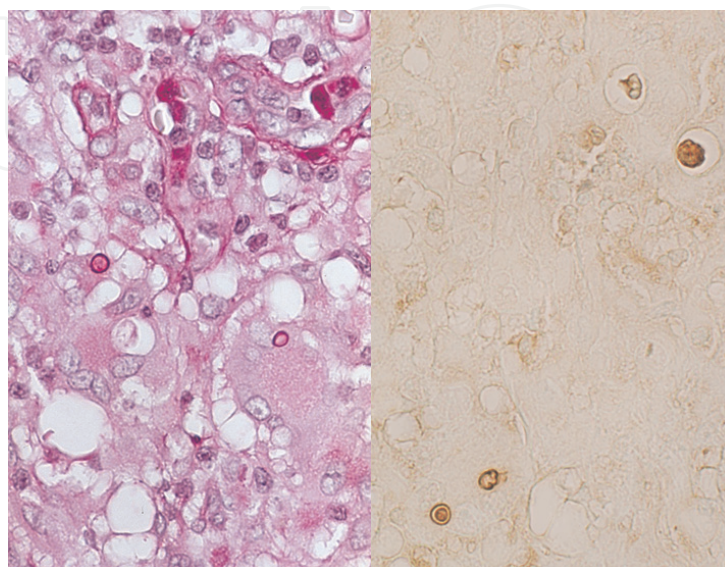

Figure 26.
Sporotrichosis (left, periodic acid-Schiff reaction; right, reactivity with patient's own serum). Suppurative granulomas are formed in the dermis. Periodic acid-Schiff-reactive small yeast-like fungal cells are phagocytized by macrophages or multinucleated giant cells and are reactive with the patient's own serum.
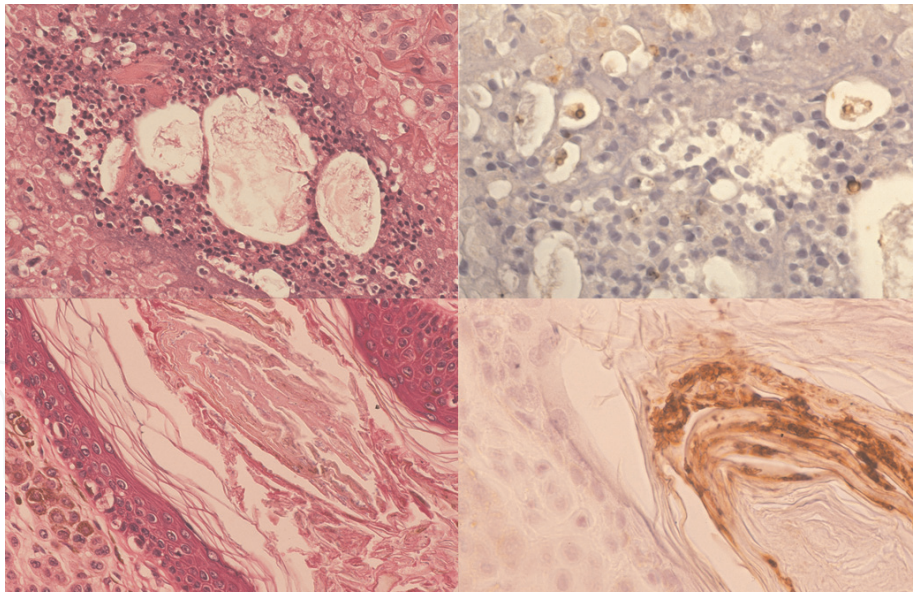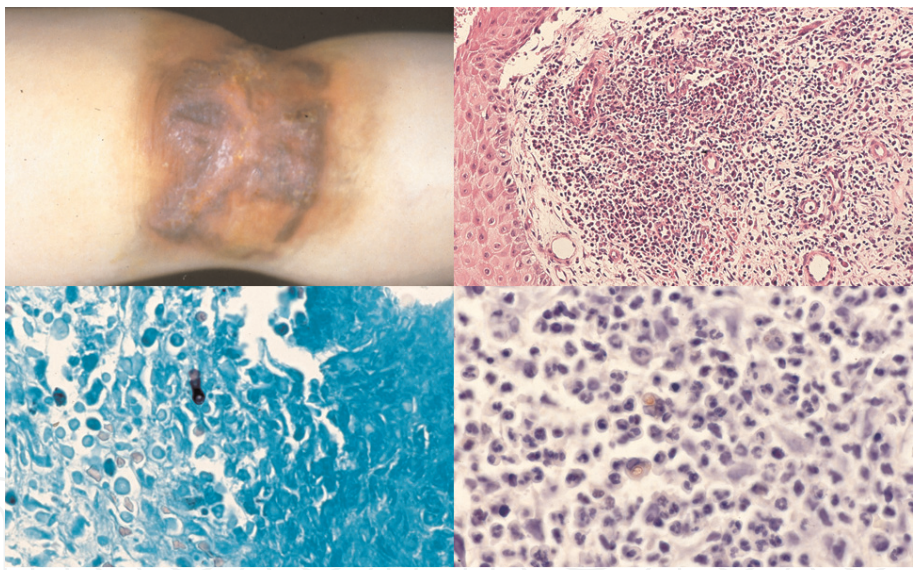
Figure 27.
*Malassezia (*Pityrosporum*) folliculitis and commensal fungi in the hair follicle (upper panels, malassezial folliculitis; lower panels, a commensal in a normal hair follicle adjacent to intradermal nevus; left, H&E; right, reactivity with patient's serum). A dilated hair follicle in biopsy material is disrupted by suppurative granuloma formation. The patient's own serum reacted with yeast-like fungi infected in the lesion. Commensal malassezial cells in the hair follicle of normal seborrheic skin, sampled from another individual, are strongly labeled with the same serum.*

Figure 28.
Cutaneous alternariosis (left upper, gross appearance of the elbow; right upper, H&E; left lower, Grocott stain; right lower, reactivity with patient's own serum). Biopsy specimen from the brown-colored skin infiltrate contains a few Grocott-reactive fungi, Alternaria alternata, *in the chronically inflamed dermis. The patient's own serum visualizes the fungal microbes phagocytized by macrophages.*

administration against acute lymphoblastic leukemia. Transparent yeasts were floating in mucoid material, and inflammatory reaction was poor. The patient's own serum diluted at 1:10 was weakly reactive to the pathogen (**Figure 29**) [20, 21, 23].

5.2.3 Viral infection

5.2.3.1 Hemorrhagic varicella

Biopsy was taken from the vesicular skin lesion of lethal hemorrhagic varicella (small pox). The patient was a young boy suffering from intractable acute
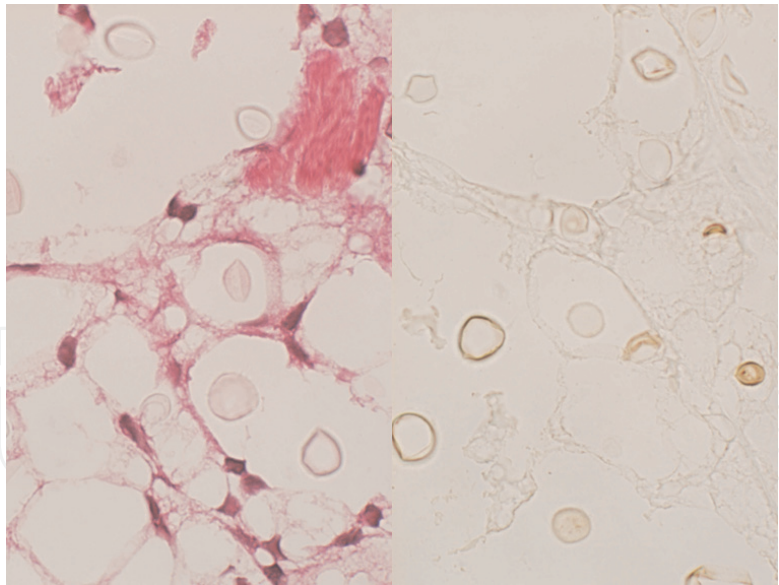
Figure 29.
Cutaneous cryptococcosis (left, H&E; right, reactivity with patient's own serum). Opportunistic skin infection of Cryptococcus neoformans *in a treated leukemia case of the young microscopically reveals transparent yeasts floating in mucoid material. Inflammatory reaction is poor. The patient's own serum diluted at 1:10 weakly reacts to the pathogen.*

lymphoblastic leukemia treated with chemotherapy and bone marrow transplantation [52]. The 1:500 diluted serum of another adult patient with a recent history of varicella clearly reacted to the plasma membrane of acantholytic keratinocytes with intranuclear viral inclusion bodies, and the localization pattern was comparable with that of GP-1 antigen revealed by immunostaining using monoclonal antibody C90.2.8 (**Figure 30**) [21, 23]. The viral intranuclear inclusions remained unreactive. It is evident that antibodies raised in the infected patient were specific to GP-1 antigen of varicella-zoster virus, an immunodominant viral substance [53].
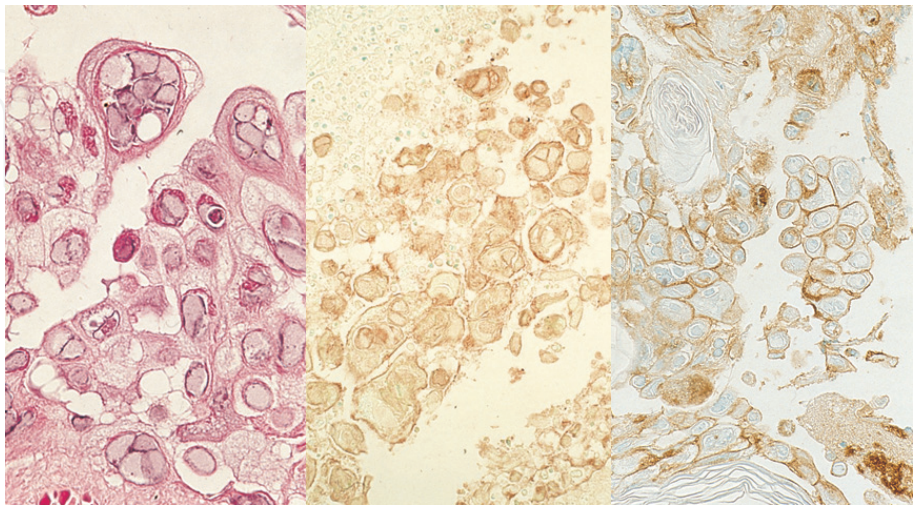

Figure 30.
Hemorrhagic varicella (left, H&E; center, reactivity with the serum of another patient; right, reactivity with monoclonal antibody C90.2.8 to GP-1 antigen of varicella-zoster virus). Biopsy was taken from a hemorrhagic vesicle, as lethal manifestation of opportunistic varicella-zoster virus infection in a leukemic boy after bone marrow transplantation. The diluted serum of another adult patient with a recent history of varicella clearly reacts to the plasma membrane of acantholytic keratinocytes with unreactive intranuclear viral inclusion bodies. The localization pattern is comparable with that of GP-1 antigen.

5.2.4 Protozoan infection

5.2.4.1 Cutaneous leishmaniasis

Figure 31 demonstrates microscopic biopsy features of African-type cutaneous leishmaniasis (*Leishmania major* infection) [54]. Japanese men, a group of 5, volunteered afforestation on the Saharan dessert in the Republic of Mali. Multiple ulcers were formed on the arms of all the members of the group. At the end of the work day, a large swarm of sandflies rushed at them. In a Japanese hospital, biopsy was taken from an ulcer on the arm of one of the members. The dermis was heavily infiltrated by macrophages full of granular microbes. The patient's own serum clearly demonstrated round pathogens in the cytoplasm of macrophages. In the biopsied older lesion seen in his friend, fewer pathogens were identified with immunostaining using the same serum [4, 8, 20–23].

Another form of cutaneous leishmaniasis, Indian type, is caused by *L. tropica* [55]. Solitary ulcer formation on the skin is characteristic of this clinical form. An aged Japanese patient stayed in India for months, and skin biopsy was performed in a Japanese hospital. Round pathogens were visualized in the cytoplasm of macrophages in the dermis by the patient's own serum (**Figure 32**) [22, 23]. Of note is that no cross-reactive staining was noted between the African and Indian types. Namely, the patient serum showed a very high specificity to the respective types of cutaneous leishmaniasis.

5.2.4.2 Acanthamebic keratitis

Acanthamebic keratitis is sight-threatening infection of the cornea by the genus *Acanthamoeba*, mostly seen in contact lens wearers [56]. A young male aged 10's, a soft contact lens user, complained of eye pain, and under the diagnosis of acanthamebic keratitis, superficial keratectomy was done. *Acanthamoeba* spp. was cultured. As shown in **Figure 33**, acanthamebic cysts and some trophozoites were identified in the corneal stroma by immunostaining using both the diluted serum of a patient of acanthamebic meningoencephalitis (see **Figure 49**) and a monoclonal
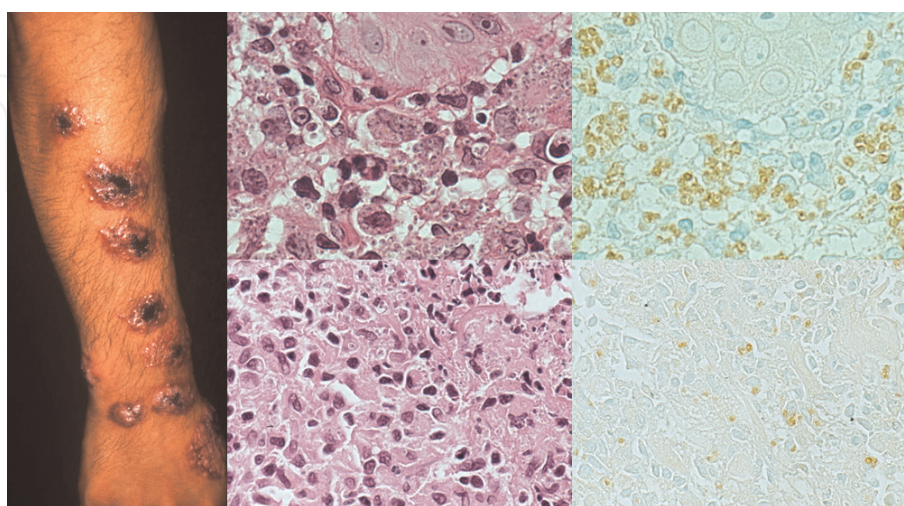

Figure 31.
*African-type cutaneous leishmaniasis (left, gross appearance of the forearm; upper panels, the patient of gross photograph; lower panels, an older lesion of his friend; center, H&E; right, reactivity with patient's serum). The Japanese men volunteered afforestation on the Saharan dessert in the Republic of Mali. Biopsy was taken from ulcerated skin lesions. The patient's own serum demonstrates round pathogens (*Leishmania major*) in the cytoplasm of macrophages infiltrating in the dermis (upper panels). In the older lesion seen in his friend (lower panels), fewer pathogens are observed with immunostaining employing the same serum.*
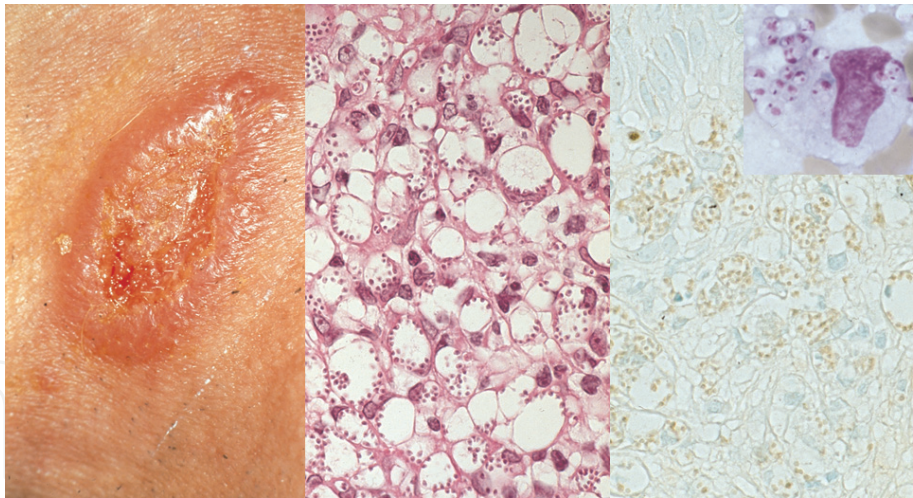
Figure 32.
Indian-type cutaneous leishmaniasis (left, gross appearance of the neck; center, H&E; right, reactivity with patient's own serum; inset, Giemsa stain on a stamp cytology preparation). Solitary skin ulcer is characteristic of this clinical form endemic in India. Biopsy specimen from a Japanese patient shows numerous round pathogens (Leishmania tropica) in the cytoplasm of macrophages in the dermis. The diluted patient's own serum visualizes the pathogen. Giemsa preparation demonstrates a pair of the nucleus and kinetoplast (smaller dot) in the protozoan cell.
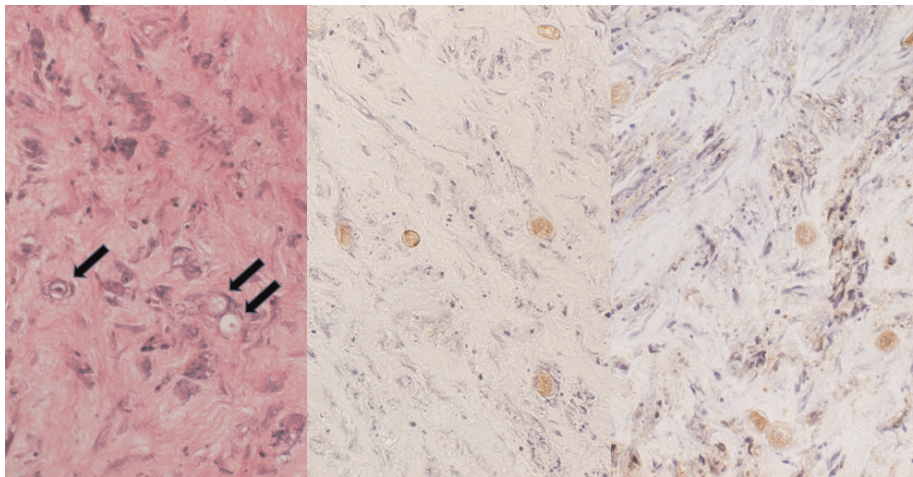

Figure 33.
Acanthamebic keratitis (left, H&E; center, reactivity with the serum of patient of acanthamebic meningoencephalitis; right, reactivity with monoclonal antibody ACA5 to Acanthamoeba sp.). Superficial keratectomy specimen from a young contact lens wearer reveals scattered amebic cysts (arrows) in the corneal stroma, and the microbes (cysts) are visualized by immunostaining using both the diluted patient's serum and the monoclonal antibody.

antibody ACA5 to *Acanthamoeba* spp. (a gift from Prof. Hiroshi Tachibana, Department of Infectious Diseases, Tokai University School of Medicine, Isehara) [57].

5.2.4.3 Amebic dysentery

Amebic dysentery, colonic infection of *Entamoeba histolytica*, is endemic in areas with poor sanitation and is often associated with AIDS [58]. Surgically resected colon specimen from an HIV-negative Japanese male patient demonstrated amebic trophozoites invading the ulcerated colon wall. As shown in **Figure 34**, the patient's own serum visualized the pathogen, and the localization was comparable with immunostaining using a monoclonal antibody EHK153 to *E. histolytica* (a gift from Prof. Yuji Tachibana, Department of Infectious Diseases, Tokai University School of Medicine, Isehara) [4, 20–23].
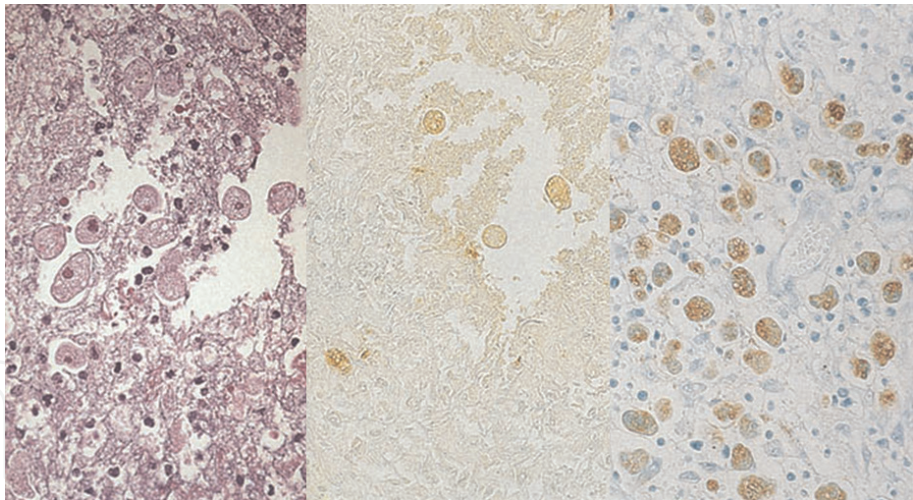
Figure 34.
Amebic dysentery (left, H&E; center, reactivity with patient's own serum; right, reactivity with monoclonal antibody EHK153 to E. histolytica). *Surgically resected colon specimen from an HIV-negative Japanese male demonstrates amebic trophozoites invading the ulcerated colon wall. The patient's own serum visualizes the pathogen, and the localization was comparable with immunostaining using the monoclonal antibody.*

5.2.4.4 Toxoplasmosis

Cryptogenic and asymptomatic infection of *Toxoplasma gondii* is common throughout the world. In patients with compromised immune system, particularly in AIDS, the parasite is activated, resulting in lethal *Toxoplasma* encephalitis. When primary infection occurs in pregnant women without serum antibody, the placental tissue is infected, causing congenital toxoplasmosis in the fetus [59]. Ruptured protozoan cysts of AIDS-associated cerebral toxoplasmosis were reactive with the serum from a healthy individual serologically with high-titer IgG. The same serum decorated trophozoites of *T. gondii* dispersed in the meningeal space in an aged HIV-negative female with progressive supranuclear palsy, confirming the diagnosis of *Toxoplasma* meningitis (**Figure 35**) [21, 22].
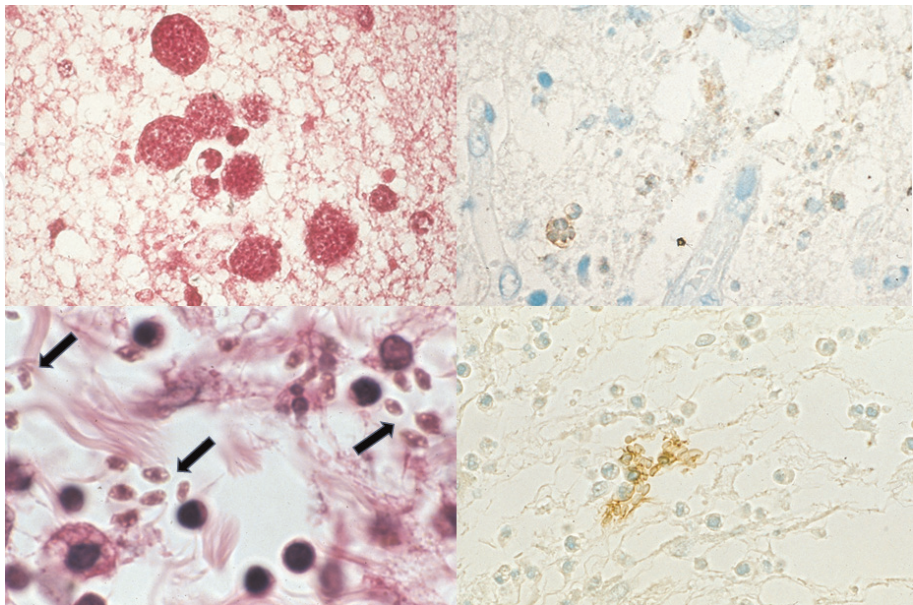

Figure 35.
Toxoplasmosis (upper panels, toxoplasma encephalitis in AIDS; lower panels, toxoplasma meningitis in a non-AIDS patient; left, H&E; right, reactivity with the serum from a healthy individual serologically with high-titer IgG). Ruptured protozoan cysts in AIDS-associated cerebral toxoplasmosis are reactive with the serum. The same serum decorates trophozoites of Toxoplasma gondii *(arrows) dispersed in the meningeal space in an aged HIV-negative female with progressive supranuclear palsy.*

5.2.4.5 Cryptosporidiosis

Cryptosporidiosis is zoonotic and waterborne infection of *Cryptosporidium parvum*, preferentially involving small bowel mucosa. In immunocompetent individuals, self-limiting watery diarrhea occurs, while in AIDS patients, the infection provokes life-threatening intractable diarrhea without effective therapeutic agents in hand [60]. The high-titer patient serum was chosen from a stock of 1994 mass infection of *C. parvum* due to contamination in the water supply system, taking place in Hiratsuka, Kanagawa, Japan. Biopsy was performed from the terminal ileal mucosa of high school boy who complained of severe diarrhea after close contact with cows in a Hokkaido farm during the summer vacation. A Japanese AIDS patient died of intractable diarrhea, and autopsy revealed cryptosporidiosis on the small bowel mucosa. Immunostaining using the high-titer serum clearly demonstrated small dot-like positive signals along the brush border of the small bowel mucosa of both patients (**Figure 36**) [21–23].

5.2.4.6 Cystoisosporiasis

Cystoisospora (formerly called *Isospora*) *belli* infection causes intractable diarrhea in individuals who live in or have traveled to tropical poor sanitary areas. Infection in immunocompromised patients, particularly AIDS patients in Africa, is life-threatening [61]. *C. belli*-induced acalculous cholecystitis is a noteworthy finding [62]. Duodenal biopsy specimen was taken from a Japanese male patient with adult T-cell leukemia in Kyushu Island. Chronic active inflammation with villous atrophy represented intractable diarrhea seen in this patient. Large-sized schizonts of *C. belli* were observed among the columnar cells in H&E preparations, and they were visualized by immunostaining using the patient's own serum (**Figure 37**) [21, 23].

5.2.4.7 Blastocystosis

Blastocystis hominis belongs to an anaerobic parasite of uncertain taxonomy found in the human digestive tract, causing diarrhea when heavily infected. Vacuolated
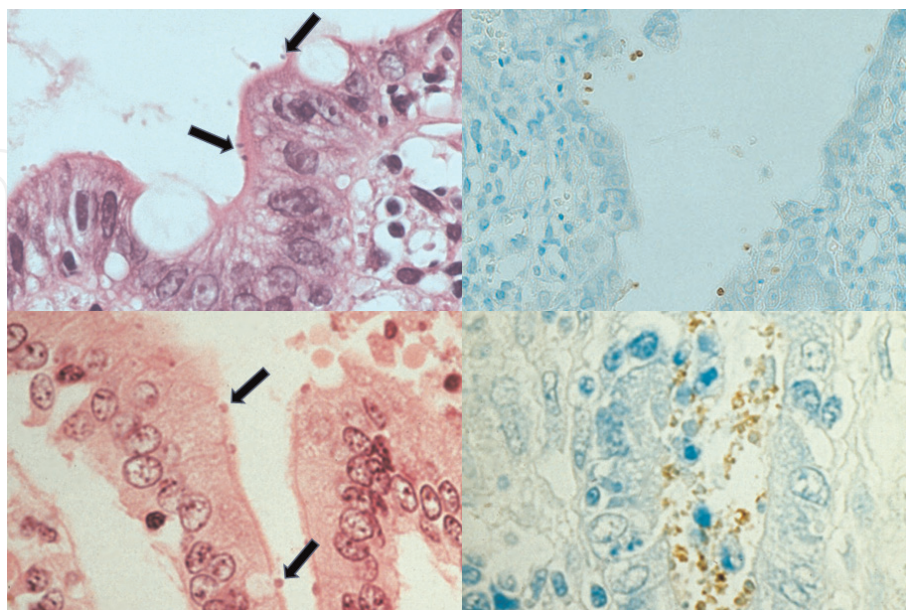

Figure 36.
Cryptosporidiosis (upper panels, ileal mucosal biopsy from a young suffering from severe diarrhea after close contact with cows in a Hokkaido farm; lower panels, autopsied jejunum of an AIDS patient complaining of lethal diarrhea; left, H&E; right, reactivity with the serum of a cryptosporidiosis patient with high-titer IgG). The tiny microbes grow in the brush border of enterocytes (arrows). Immunostaining using the high-titer serum demonstrates dot-like positive signals on the apex of the columnar cells of both patients.
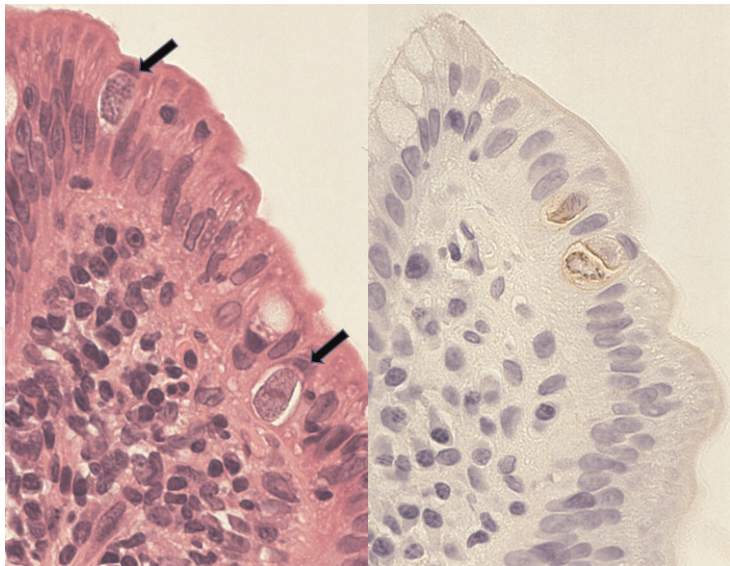
Figure 37.
Cystoisosporiasis (left, H&E; right, reactivity with patient's own serum). Duodenal biopsy specimen was taken from a Japanese male patient with adult T-cell leukemia in Kyushu Island, complaining of severe diarrhea. Large-sized schizonts of Cystoisospora belli *are scattered among the columnar cells (arrows). Immunostaining using patient's own serum decorates the microbe.*

morphology and size variation are characteristic [63]. We encountered a patient with diarrhea and high-titer serum antibody to *B. hominis* [64]. The target of immunostaining was formalin-fixed, paraffin-embedded cell block preparations of cultured *B. hominis*. Cell wall positivity was clearly observed, as shown in **Figure 38** [21–23].

5.2.5 Helminthic infection

5.2.5.1 Gnathostomiasis

Infestation of *Gnathostoma* happens after eating undercooked or raw freshwater fish, frogs, birds, and reptiles, and migratory swelling of the skin (creeping disease) follows [65]. Cut surface of *G. hispidum* was identified in targeted abdominal skin biopsy from creeping disease, seen in a Japanese male patient aged 60's. The larval body is histologically featured by spiculated cuticles, well-developed muscle cells
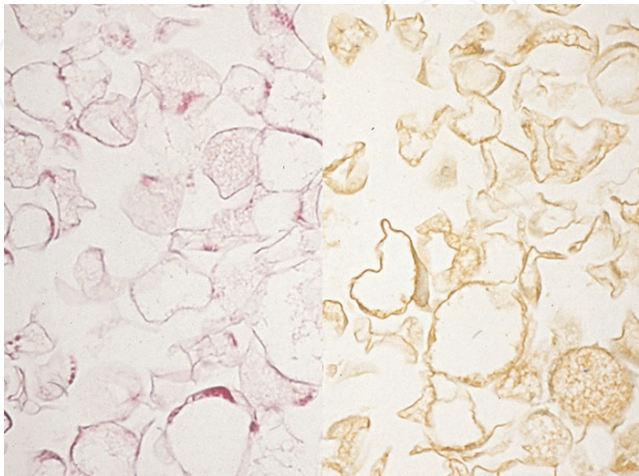

Figure 38.
Blastocystosis (cultured Blastocystis hominis *in cell block preparation: left, H&E; right, reactivity with the serum of a patient with serologically proven high-titer IgG). Cultured* B. hominis *reveals vacuolated morphology and size variation. The centrifuged pellet was fixed in formalin and embedded in paraffin to prepare cell blocks. The cell wall of the microbes is immunostained with the serum of a patient with diarrhea and high-titer serum antibody to* B. hominis.
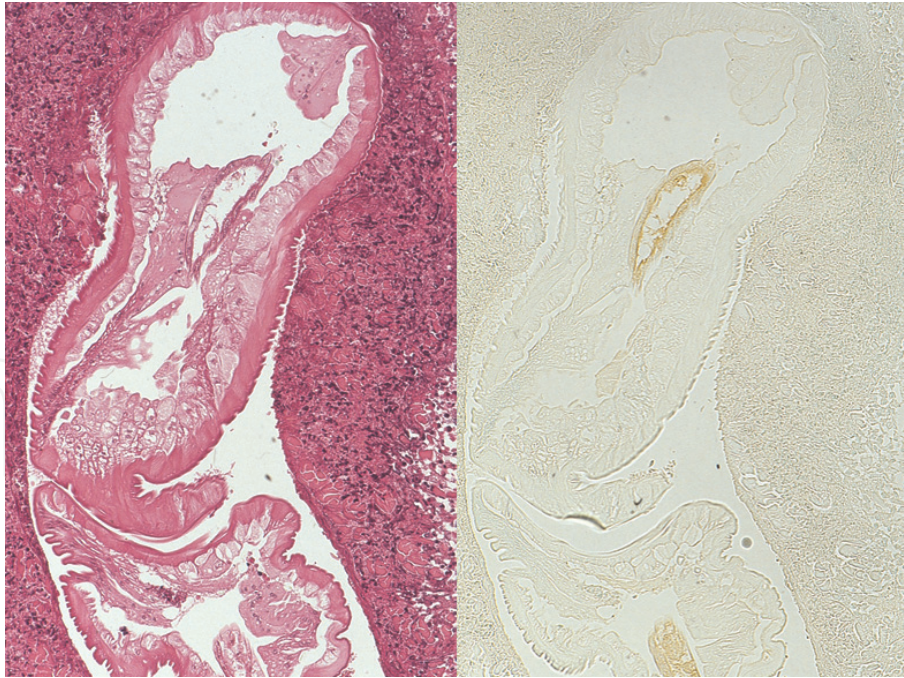
Figure 39.
Gnathostomiasis (left, H&E; right, reactivity with patient's own serum). A Japanese male manifested creeping disease on the abdomen. Targeted biopsy reveals cut surfaces of Gnathostoma hispidum *in the dermis. The larval body is histologically featured by spiculated cuticles, well-developed muscle cells with clear cytoplasm, eosinophilic lateral chords, and the centrally located gut. The patient's serum was solely reactive with the gut cells.*

with clear cytoplasm, eosinophilic lateral chords, and the centrally located gut. The patient's serum was solely reactive with the gut cells (**Figure 39**) [21, 23].

5.2.5.2 Ectopic anisakiasis

Anisakis species belongs to a dolphin/whale ascarid. Anisakiasis is caused by the ingestion of a larval nematode in raw seafood dishes such as sushi and sashimi. Infestation occurs mainly in the stomach, but infrequently intestinal or extra-gastrointestinal anisakiasis is encountered [66]. A dead and decayed larval nematode was identified in the peritoneal (omental) nodule, and microscopic identification of the nematode species was impossible. The diagnosis of extra-gastrointestinal anisakiasis was made by distinct immunoreactivity with a monoclonal antibody An2 against *Anisakis simplex* (a gift from late Dr. Hajime Ishikura, Sapporo Medical University, Sapporo). The 1:500 diluted patient's own serum reacted weakly with the internal organs, especially the gut (**Figure 40**) [21].

5.2.5.3 Schistosomiasis japonicum

Schistosomiasis is caused by digenetic blood trematodes (fluke). Water snail-mediated three main species infest humans: *Schistosoma japonicum*, *S. haematobium*, and *S. mansoni*. Larvae (cercariae) show percutaneous infestation through intact skin. Paired adult worms of *S. japonicum* fix to the portal vein and provoke liver cirrhosis. The disease, rampant until the 1960s in certain areas of Japan, has been eradicated by 1976 [67]. Now, Mainland China and the Philippines are the main countries of epidemic [68]. We occasionally experience aged Japanese people accompanying calcified ova in the liver and colon. **Figure 41** demonstrates biopsied colonic mucosa with acid-fast *Schistosoma* ova in an aged asymptomatic male living in Kofu Basin, the historical endemic area. The patient's serum diluted at 1:200 reacted with the shell of the ovum [21].
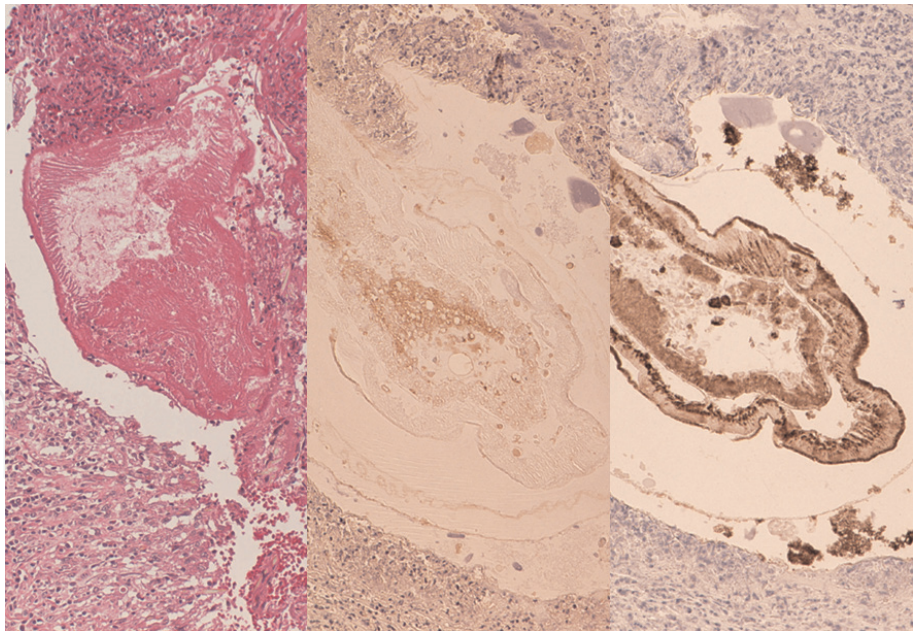
Figure 40.
Ectopic anisakiasis (left, H&E; center, reactivity with patient's own serum; right, reactivity with monoclonal antibody An2 to Anisakis simplex*). A dead and decayed larval nematode is seen in the omental nodule, and the diagnosis of extra-gastrointestinal anisakiasis was made by distinct immunoreactivity with the monoclonal antibody. The diluted patient's own serum reacts weakly with the internal organs, especially the gut.*
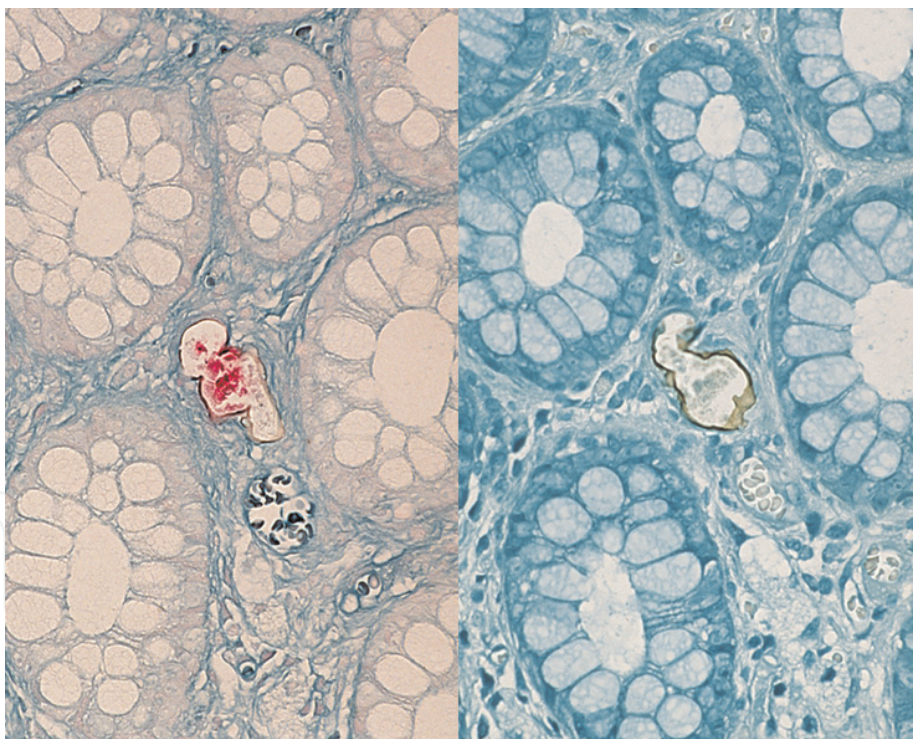

Figure 41.
Schistosomiasis japonicum (left, acid-fast staining; right, reactivity with patient's own serum). In biopsied colonic mucosa of an asymptomatic individual living in a historical endemic area, acid-fast ova of Schistosoma japonicum *are observed in the lamina propria mucosae. The patient's serum diluted at 1:200 reacts with the shell of the ovum.*

5.2.5.4 Bilharziasis

Schistosoma haematobium infestation (bilharziasis) is endemic in sub-Saharan African continent. Infection occurs in fresh water in a short time (just for 10 min) when a larval form (cercaria) of *S. haematobium*, developing in the fresh water

snail, penetrates the intact skin. Paired adult worms, 1.5–2 cm in size, settle in para-vesicular pelvic veins, and ova are excreted from ulcers formed in the urinary bladder to the urine [69]. Ectopic egg tubercles (foreign body granulomas against eggs) may be formed in the uterine cervix, ureter, and rectosigmoid colon and even in the brain. Two young Japanese male patients with a history of staying in African continent complained of hematuria and presented ectopic egg tubercles in the sigmoid colon and in the brain, respectively. The multinucleated (miracidial) content of the egg was strongly labeled with the patient's own serum in both the biopsied colon and surgically resected cerebral lesion (**Figure 42**) [21, 23].

5.2.5.5 Multilocular echinococcosis

Multilocular (alveolar) echinococcosis, infestation of *Echinococcus multilocularis*, is endemic in Hokkaido, the northernmost island of Japan. This zoonotic parasitosis showing liver involvement is mainly mediated by ingestion of eggs excreted from red foxes [70]. The liver infested by *E. multilocularis* was surgically removed from a female patient aged 30's living in Hokkaido. The multilocular hydatid cyst wall was collapsed and embedded in the fibrous tissue. No protoscolex was seen in the lesion. The patient's serum diluted at 1:200 was reactive with the collapsed cyst wall component, while the intact hydatid cyst wall revealed negativity (**Figure 43**) [23].

5.2.5.6 Neurocysticercosis

Neurocysticercosis is infestation of *Cysticercus cellulosae*, a larval form of *Taenia solium* (tapeworm). Infestation occurs by ingesting *C. cellulosae* embedded in raw pork or eggs in contaminated food [71]. The brain lesion of larva migrans in a young Japanese female was surgically removed. A cysticercus body with scolex formation was microscopically lined by eosinophilic tegument and underlying subcuticular cells. The patient's serum was weakly reactive with the tegument (**Figure 44**) [21, 23].
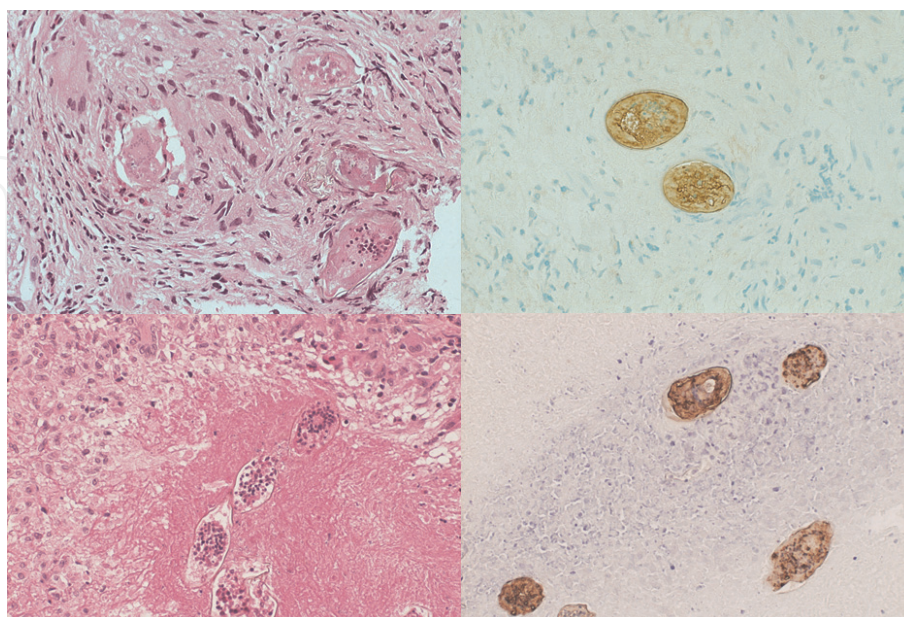

Figure 42.
Bilharziasis (upper panels, egg tubercle in the sigmoid colon; lower panels, surgical material of brain lesion; left, H&E; right, reactivity with patient's own serum). Two young Japanese male patients with a history of staying in African continent complained of hematuria and presented ectopic egg tubercles in the sigmoid colon and in the brain, respectively. The multinucleated (miracidial) content of the egg of Schistosoma haematobium *is strongly reactive with the patient's own serum in the respective lesions.*
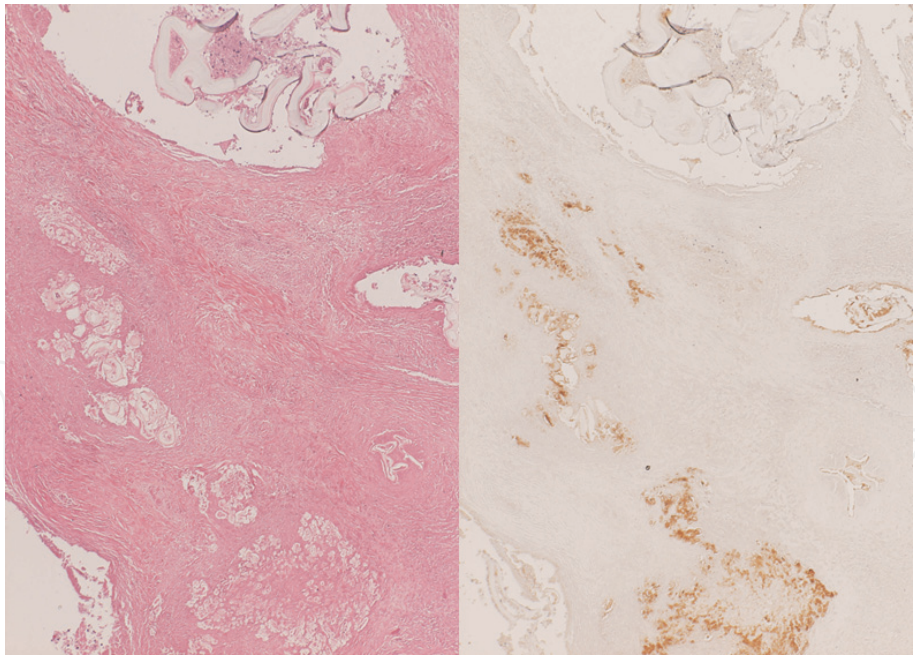
Figure 43.
Multilocular echinococcosis (left, H&E; right, reactivity with patient's own serum). The liver infested by Echinococcus multilocularis *was surgically removed from a female patient living in Hokkaido. The multilocular hydatid cyst wall has been collapsed and embedded in the fibrous tissue. The patient's serum is reactive with the collapsed cyst wall component, while the intact hydatid cyst wall reveals negativity.*
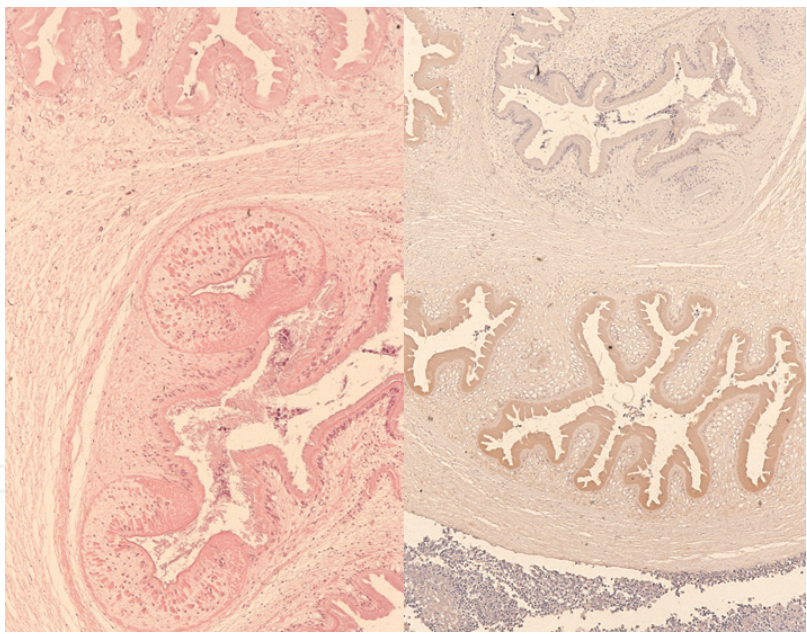

Figure 44.
Neurocysticercosis (left, H&E; right, reactivity with patient's own serum). The brain lesion of larva migrans in a Japanese female was surgically removed. A cysticercus body with scolex formation is microscopically lined by eosinophilic tegument and underlying subcuticular cells. The patient's serum is weakly reactive with the tegument.

5.3 Immunostaining using the serum of patients without fixed diagnosis

When the diagnosis is unsettled, the specificity of the patient's serum remains unknown. If the positive signals reactive with the patient's serum are seen within the inflammatory lesion, it is reasonable for us to regard that the target microbes are visualized. The size and shape of the stained targets suggested certain causative pathogens within the lesion [20–23]. The final diagnosis can be made by combining

35

clinical information and histopathological appearance with the morphology of the pathogen. Of no doubt, this gives us the most powerful and useful situation in applying immunostaining using the patient serum.

5.3.1 Propionibacterium acnes folliculitis

Invasive opportunistic infection of *Propionibacterium acnes*, a commensal in the hair follicle, has been described [72]. An aged afebrile Japanese male complained of a skin nodule on the chest. Biopsy revealed hair follicle-centered inflammation, and macrophages clustered around the hair follicle contained numerous granular-looking microbes. Microscopically, the possibility of yeast-form mycosis, rickettsiosis, and protozoan infection was suspected. Grocott positivity was faint. Immunostaining using *B. cereus* antiserum revealed positivity (see **Figure 22**), while antisera to BCG, *T. pallidum*, and *E. coli* did not. The patient's own serum diluted at 1:500 clearly demonstrated the pathogen not only in macrophages but also in commensal bacterial colonies in the hair follicle [23]. Finally, PAC3 antigen specific to *P. acnes* was positive (through the courtesy of Prof. Yoshinobu Eguchi, Department of Pathology, Tokyo Medical and Dental University, Tokyo) [73], and the diagnosis of *P. acnes*-induced folliculitis was thus confirmed (**Figure 45**).

5.3.2 Ectopic liver infestation of Ascaris lumbricoides

Ectopic infestation of *Ascaris lumbricoides* in the hepatobiliary tract has been reported [74]. A farmer housewife aged 40's complained of abdominal pain. Liver abscess was indicated by diagnostic imaging, and partial hepatectomy specimen revealed multiple yellow-colored xanthogranulomatous nodules at the liver hilus. Microscopically, a small number of dead and calcified ova were distributed in necrotic substance, while the parasite body had been absorbed [75]. The content of the ova was immunoreactive with the diluted patient's serum [7, 20, 21, 23, 75]. Ouchterlony's diffusion-in-gel test using the extract of varied helminths identified a
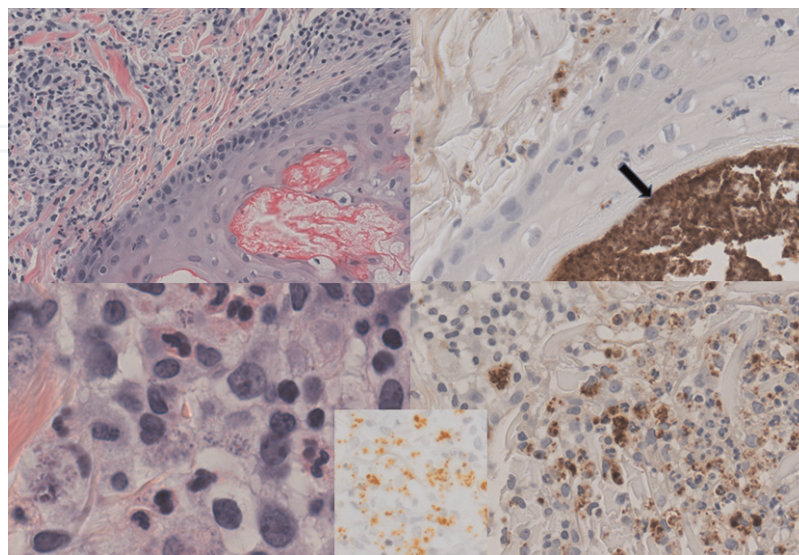

Figure 45.
Propionibacterium acnes *folliculitis (upper panels, dilated hair follicle with histiocytic reaction in the perifollicular dermis; lower panels, higher powered view of the infiltrating macrophages; left, H&E; right, reactivity with patient's own serum; inset, immunostaining for PAC3 antigen specific to* P. acnes*). Macrophages clustered around the dilated hair follicle contain numerous granular-looking microbes. The patient's own serum clearly demonstrates the pathogen not only in macrophages but also in commensal bacterial colonies in the hair follicle (arrow). Immunostaining for PAC3 antigen confirms the diagnosis of* P. acnes-*induced folliculitis.*
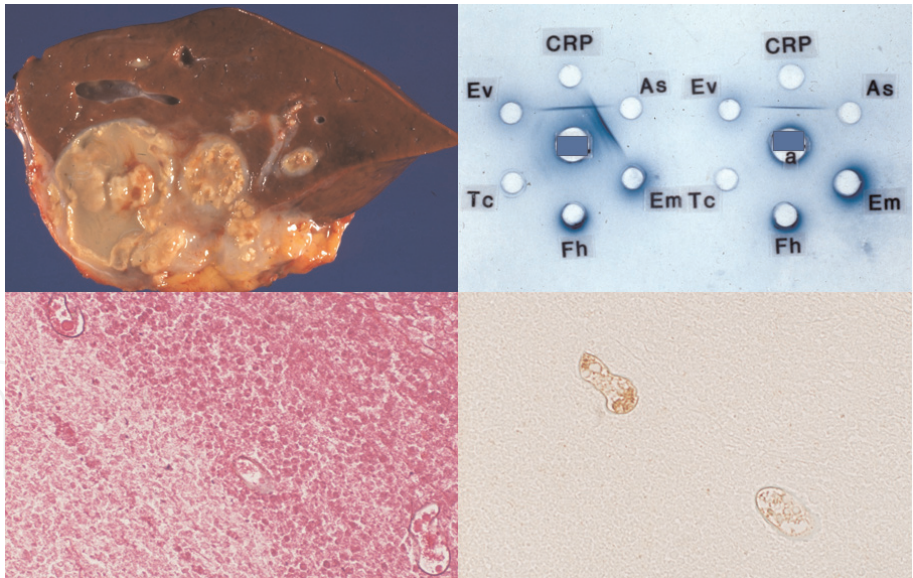
Figure 46.
Hepatic ascariasis (left upper, cut surface of the resected liver; right upper, Ouchterlony's diffusion-in-gel test using the extract of varied helminths; left lower, H&E; right lower, reactivity with patient's own serum). Yellow-colored xanthogranulomatous nodules are seen at the liver hilus. Microscopically, a small number of dead and calcified ova are distributed in necrotic substance. The content of the ova is immunoreactive with the patient's serum. In Ouchterlony's test, a precipitation line against Ascaris lumbricoides *(As) has been absorbed by the* Ascaris *extract, as shown on the right hand (Em, Echinococcus multilocularis; Fh, Fasciola hepatica; Tc, Toxocara canis; EV, Enterobius vermicularis; CRP, C-reactive protein).*

clear precipitation line against *A. lumbricoides* (**Figure 46**). The precipitation line was abolished by preabsorbing the serum with the roundworm extract [75]. The final diagnosis was ectopic ascariasis, caused by infestation of a young (immature) female worm. The serum was unreactive with ova of *Schistosoma japonicum* and *Paragonimus miyazakii* seen in paraffin sections. The inner surface of the cell wall of *A. simplex* larva was weakly stained with the serum [21].

Figure 47 demonstrates a splenic lesion with ectopic migration of *A. lumbricoides*. Necrotizing granulomas were formed beneath the splenic capsule, and dead parasite body fragments were seen in the necrotic area. It was impossible to determine the species of nematode under microscopy. The abovementioned serum
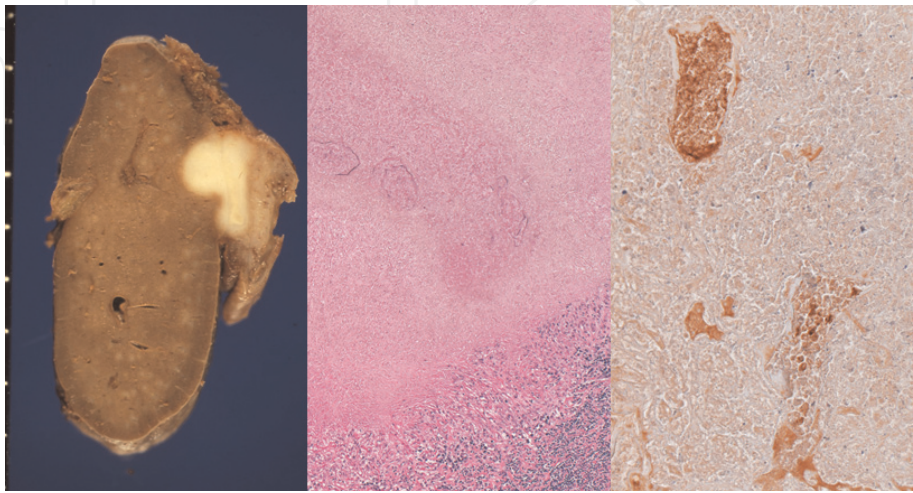

Figure 47.
Splenic ascariasis (left, cut surface of the formalin-fixed spleen; center, H&E; right, reactivity with the serum of patient with hepatic ascariasis). Ectopic migration of A. lumbricoides *has provoked necrotizing granulomas beneath the splenic capsule. Dead parasite body fragments are seen in the necrotic area. The abovementioned serum of patient with hepatic ascariasis reacts with the dead worm body, confirming the diagnosis of ectopic splenic ascariasis.*

of patient with hepatic ascariasis reacted with the dead worm body, confirming the diagnosis of ectopic splenic ascariasis. The serum functioned as an immunohistochemical probe specific to *A. lumbricoides* [21].

5.3.3 Visceral leishmaniasis

Visceral leishmaniasis, sandfly-mediated systemic infection of *Leishmania donovani*, kills more than 20,000 persons in 2015 but has been classified by the World Health Organization as a neglected tropical disease [76]. A Japanese businessman aged 30's stayed in a sequential order in Australia, Thailand, Singapore, and finally India [77]. During his stay in India, he manifested headache, high fever, thrombocytopenia, and liver dysfunction. The patient was hospitalized in Japan, but his general condition was poor. In order to confirm the diagnosis, liver biopsy was performed. Small epithelioid granulomas were identified, and the possibility of Q fever in Australia, melioidosis in Thailand, brucellosis, miliary tuberculosis, and non-tuberculous mycobacteriosis was considered histopathologically. No positive findings were obtained in immunohistochemical analysis using a panel of antibodies. The patient's own serum diluted at 1:500 demonstrated red cell-sized positive signals in the cytoplasm of epithelioid cells (**Figure 48**) [7, 8, 21, 23, 77]. The size and shape of the pathogen strongly suggested visceral leishmaniasis (kala azar) endemic in India. High serum immunofluorescence titer against *L. donovani* was serologically confirmed thereafter. Administration of pentavalent antimony compound saved his life. This is the real case, in which immunostaining using the patient's own serum was practical maximally.

5.3.4 Free-living amebic meningoencephalitis

Free-living amoeba widely seen in soil and water may cause lethal meningoencephalitis as an opportunistic or non-opportunistic infection [78]. A Japanese male
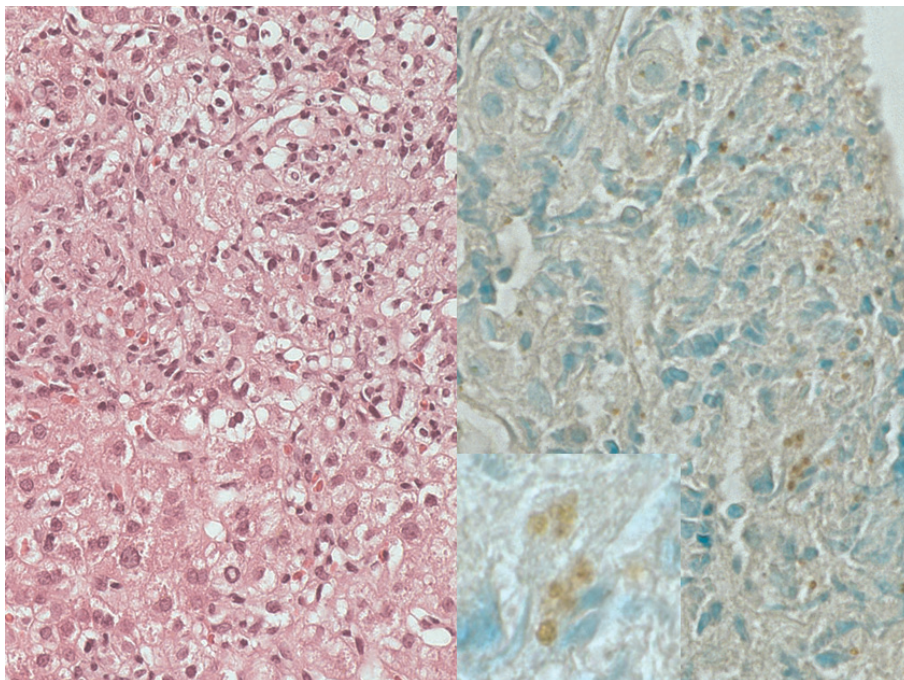

Figure 48.
Visceral leishmaniasis (left, H&E; right, reactivity with patient's own serum; inset, high-powered view). During the stay in India, a Japanese businessman manifested headache, high fever, thrombocytopenia, and liver dysfunction. Liver biopsy shows small epithelioid granulomas. A panel of immunohistochemical analysis has failed to identify the causal agent. The patient's own serum demonstrates red cell-sized positive signals in the cytoplasm of epithelioid cells, strongly suggesting visceral leishmaniasis (kala azar) endemic in India. The final diagnosis was made by the serological study and successful treatment.

aged 60's suffering from alcoholic liver cirrhosis manifested left hemiparesis [79]. Computed tomography disclosed multifocal low densities in his right hemisphere. Herpetic encephalitis was clinically suspected. HIV antibody was negative. Progressive intracranial edema necessitated decompressive craniotomy with brain biopsy. The brain tissue microscopically showed perivascular chronic active inflammation, with ameba-like cells somewhat resembling macrophages being scattered. The 1:500 diluted patient's serum clearly reacted with the protozoan bodies, and mouse antiserum to *Acanthamoeba culbertsoni* (a gift from Prof. Yuji Tachibana, Department of Infectious Diseases, Tokai University School of Medicine, Isehara) also gave positivity (**Figure 49**) [7, 8, 21, 23, 77]. No reactivities for *A. polyphaga* and *A. castellanii* were noted. High immunofluorescence titer against *A. culbertsoni* was serologically confirmed in the patient's serum. Detailed microscopic observation of H&E-stained preparations disclosed the presence of acanthamebic trophozoites and cysts in the brain tissue. The final diagnosis was opportunistic acanthamebic meningoencephalitis associated with liver cirrhosis.

Balamuthia mandrillaris may cause amebic meningoencephalitis in both immunocompromised and immunocompetent individuals [80]. An amoeba-induced skin nodule may be formed before the onset of meningoencephalitis [81]. A healthy Japanese farmer housewife aged 50's suddenly complained of progressive consciousness disturbance and seizure. She daily grew vegetables. Two weeks after onset, the patient expired. At autopsy, the basal side of the brain grossly revealed hemorrhagic meningoencephalitis. Microscopically, large-sized, basophilic amebic trophozoites were clustered mainly in Virchow-Robin's spaces. Smaller-sized cysts were focally observed. PCR analysis disclosed infection of *B. mandrillaris*. Immunostaining using both the patient's own serum and the patient's serum of the abovementioned acanthamebic meningoencephalitis gave distinct positivity (**Figure 50**) [23]. *Balamuthia*-infected skin nodule seen in another patient gave clear positivity of the microbe using these two patients' sera. Cross-reactivity of the acanthamebic antigens to *Balamuthia* species was thus confirmed, but the serum
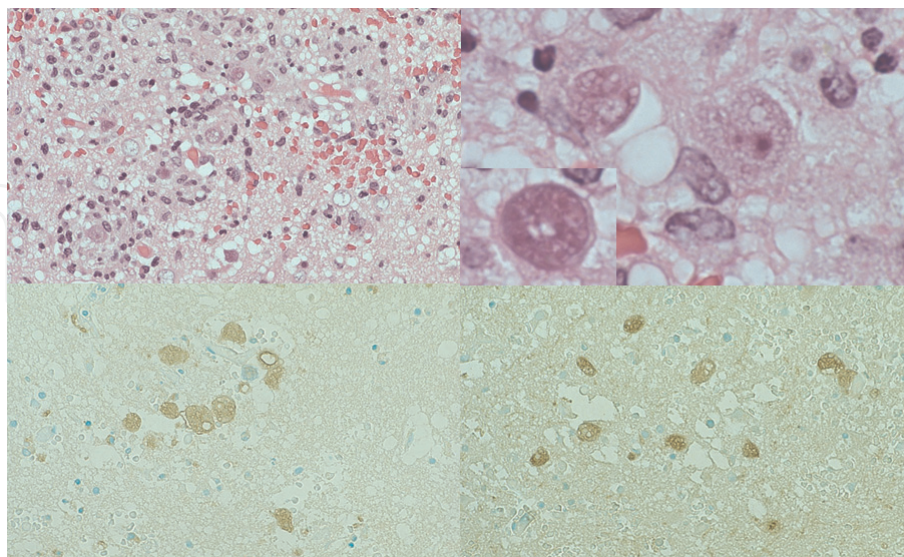

Figure 49.
Acanthamebic meningoencephalitis (left upper, low-powered H&E; right upper, high-powered H&E; inset, an amebic cyst; left lower, reactivity with patient's own serum; right lower, reactivity with mouse antiserum to Acanthamoeba culbertsoni*). An HIV-negative Japanese male suffering from alcoholic liver cirrhosis manifested left hemiparesis. Progressive intracranial edema necessitated decompressive craniotomy with brain biopsy. The brain tissue microscopically shows perivascular chronic active inflammation, and amebic trophozoites and cysts (inset) are scattered. The diluted patient's serum clearly reacts with the amebic bodies.* A. culbertsoni *infection has been confirmed by using a panel of mouse antisera against different* Acanthamoeba *subspecies.*
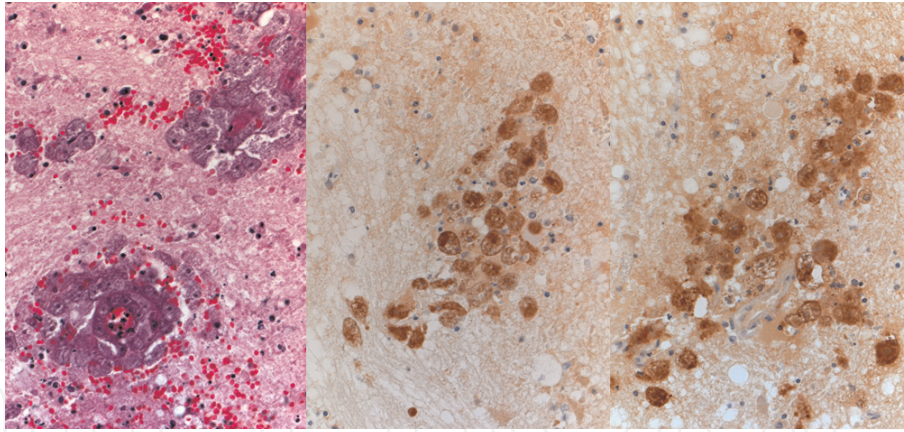
Figure 50.
Balamuthia *meningoencephalitis (left, H&E; center, reactivity with patient's own serum; right, reactivity with the serum of patient of acanthamebic meningoencephalitis). A healthy Japanese farmer housewife complained of progressive consciousness disturbance and seizure. At autopsy, hemorrhagic meningoencephalitis was observed. Large-sized, basophilic amebic trophozoites are microscopically clustered in Virchow-Robin's spaces. PCR analysis has disclosed infection of* B. mandrillaris. *Immunostaining using both the patient's own serum and the patient's serum of the abovementioned acanthamebic meningoencephalitis gives distinct positivity. Of note is that heat-induced antigen retrieval is needed for visualizing* B. mandrillaris *antigens.*

was not cross-reactive to *Naegleria fowleri* (brain-eating amoeba) seen in the autopsied brain of another patient. Regarding acanthamebic keratitis, see **Figure 33**.

Of note is an exception that *Balamuthia* antigens were detectable by the diluted patient's serum only after heating pretreatment of deparaffinized sections in 10 mM citrate buffer, pH 6. Without heat-induced antigen retrieval, signals were not observed at all. Therefore, the author strongly recommends employing the heating pretreatment for immunostaining using patients' sera in order to avoid unexpected false negativity. Silane-coated glass slides should thus be used for preventing section detachment.

6. Concluding remarks

Undoubtedly, the detection of causative pathogens in the inflammatory lesion is the key step directing to the correct histopathological diagnosis of infectious diseases. Even if the specificity of the serum is unknown, the final diagnosis can be reached, based on the morphology and distribution of the positive signals, when combined with tissue reactions, laboratory data and clinical features. In the present article, the author introduced two different approaches using low-specificity antisera. The targets were formalin-fixed and paraffin-embedded sections. One approach is the use of commercially available rabbit antisera showing wide cross-reactivity to a variety of bacteria, and another is the use of diluted patients' sera.

Immunostaining using plural antimicrobial antisera commonly yielded clear positivity with low background, because of poor cross-reactivity of bacterial antigens to human cells and tissues. The approach described here was aimed at visualizing the causative bacteria within infectious lesions in routinely prepared paraffin sections through a wide cross-reactivity shown by low-specificity rabbit antisera against four kinds of bacteria.

Immunostaining using patients' sera is also quite useful in making the histopathological diagnosis. Occasionally, IgG in the patients' sera showed cross-reactivity to related pathogens wider than expected. In bacterial and fungal infection, the sera served as pan-bacterial and pan-fungal probes, respectively. Despite such broad/low specificity, this convenient procedure is excellent in selectively identifying the pathogen within the lesion in question. In viral, protozoal, and

helminthic infection, the specificity was much narrower with limited cross-reactivities, and once the specificity is known, the patients' sera turn to become specific primary antibodies for identifying pathogens in the following new cases.

In the latter approach, what one should do is, instead of ordering an expensive antibody of unknown quality, to make a brief phone call to clinicians or laboratory technicians to ask to save a small aliquot of patients' sera, soon after microscopic confirmation of the host response in histopathology specimens. This is particularly true when specific antibodies are not listed in the commercial catalog. Of note is that informed consent is unnecessary when the patient's serum is utilized primarily for making a diagnosis of the patient's own. When the serum is applied to immunostaining for another case as the primary antibody, the author strongly recommends linking the preserved serum non-anonymously.

The author sincerely hopes that the approaches shown here will be applied to the histopathological diagnosis of infectious diseases in the readers' laboratories.

Acknowledgements

Conflict of interest

The author has no conflict of interest in the present study.

Author details

Yutaka Tsutsumi
Pathos Tsutsumi, Toyoake, Aichi, Japan

*Address all correspondence to: pathos223@kind.ocn.ne.jp

IntechOpen

References

[1] World Health Organization. Global Health Observatory (GHO) data. Top 10 causes of death. 2016. Available from: https://www.who.int/gho/mortality_burden_disease/causes_death/top_10/en/

[2] Tsutsumi Y. Atlas of Infectious Disease Pathology. Bunkodo: Tokyo; 2000. 349 p (in Japanese). Available from: http://pathos223.com/atlas/index.htm

[3] Tsutsumi Y. Pathology of Infectious Diseases. 2003. Available from: https://pathos223.com/en/

[4] Tsutsumi Y. Application of the immunoperoxidase method for histopathologic diagnosis of infectious diseases. Acta Histochemica et Cytochemica. 1994;**27**:547-560

[5] Azumi N. Immunohistochemistry and *in situ* hybridization techniques in the detection of infectious organisms. In: Connor DH, Chandler FW, Schwartz DA, et al., editors. Pathology of Infectious Diseases. Vol. I. Stamford, CT: Appleton & Lange; 1997. pp. 35-44

[6] Chandler FW. Morphology to molecular biology: Approaches to the pathologic diagnosis of infectious diseases. In: Horsburgh CR, Nelson AM, editors. Pathology of Emerging Infections. Washington DC: ASM Press; 1997. pp. 7-19

[7] Tsutsumi Y. Detection of infectious pathogens in pathology specimens. Byori-to-Rinsho. 2003;**21**:74-91 (in Japanese)

[8] Tsutsumi Y. Infectious diseases: Bacterial, fungal and protozoan infections. Byori-to-Rinsho. 2014;**32** (Extra issue: Immunohistochemistry): 306-319 (in Japanese)

[9] Tsutsumi Y. Pathology of Skin Infections. NY, USA: Nova Biomedical; 2013. 378 p. Available from: http://pathos223.com/bookintroduction/pathology_of_skin_infectious.html

[10] Tsutsumi Y. Infectious diseases. In: Fukayama M, Oda Y, Sakamoto M, et al, editors. Atlas of Histopathology, Ver. 6. Tokyo: Bunkodo; 2015. pp. 497-523 (in Japanese)

[11] Ramos-Vara JA, Miller MA. When tissue antigens and antibodies get along: Revisiting the technical aspects of immunohistochemistry—The red, brown, and blue technique. Veterinary Pathology. 2014;**51**:42-87

[12] Kabiraj A, Gupta J, Khaitan T, Bhattacharya PT. Principle and techniques of immunohistochemistry: A review. International Journal of Biological and Medical Research. 2015;**6**: 5204-5210

[13] Tsutsumi Y. Immunohistochemistry. Points of attention for specimen preparation and immunostaining. I-to-Cho. 2017;**52**:973-987 (in Japanese)

[14] Keasey SL, Schmid KE, Lee MS, et al. Extensive antibody cross-reactivity among infectious Gram-negative bacteria revealed by proteome microarray analysis. Molecular & Cellular Proteomics. 2009;**8**:924-935

[15] Murray PR, Baron EJ, Pfaller MA, et al., editors. Manual of Clinical Microbiology. 7th ed. Washington, DC: ASM Press; 1999

[16] Fujii M, Mizutani Y, Sakuma T, et al. *Corynebacterium kroppenstedtii* in granulomatous mastitis: Analysis of formalin-fixed, paraffin-embedded biopsy specimens by immunostaining using low-specificity bacterial antisera and real-time polymerase chain reaction. Pathology International. 2018; **68**:409-418

[17] Kamoshida S, Satoh Y, Kamiya S, Tsutsumi Y. Heat shock protein 60 (HSP60) immunoreactivity in gastric epithelium associated with *Helicobacter pylori* infection: A pitfall in immunohistochemically interpreting HSP60-mediated autoimmune responses. Pathology International. 1999;**49**:88-90

[18] Gonzalez-Escobedo G, La Perle KMD, Gunn JS. Histopathological analysis of *Salmonella* chronic carriage in the mouse hepatopancreatobiliary system. PLoS One. 2013;**8**(12):e84058. DOI: 10.1371/journal.pone.0084058

[19] Tsutsumi Y. Immunostaining placing more emphasis on sensitivity than specificity. Kagakuryoho-no-Ryoiki. 2018;**34**:4-20 (in Japanese)

[20] Tsutsumi Y, Kawai K, Nagakura K. Use of patients' sera for immunoperoxidase demonstration of infectious agents in paraffin sections. Acta Pathologica Japonica. 1991;**41**: 673-679

[21] Tsutsumi Y. Histopathological diagnosis of infectious diseases using patients' sera. Seminars in Diagnostic Pathology. 2007;**24**:243-252

[22] Tsutsumi Y. Histopathological diagnosis of protozoan infection using patients' sera. In: Ishikura H, editor. Host Response to International Parasitic Zoonoses. Tokyo: Springer-Verlag; 1998. pp. 69-81

[23] Tsutsumi Y. Detection of pathogens using patients' sera. Kagakuryoho-no-Ryoiki. 2018;**34**:182-199 (in Japanese)

[24] Kawai K, Tsutsumi Y. Immunoperoxidase visualization of acid-fast bacilli. A comparison with conventional acid-fast staining. Byori-to-Rinsho. 1984;**2**:862-867 (in Japanese)

[25] Wiley EL, Mulhollan TJ, Beck B, et al. Polyclonal antibodies raised against *Bacillus* Calmette-Guérin, *Mycobacterium duvalii*, and *Mycobacterium paratuberculosis* used to detect mycobacteria in tissue with the use of immunohistochemical techniques. American Journal of Clinical Pathology. 1990;**94**:307-312

[26] Tsutsumi Y. Demonstration of pathogens in archival pathology sections. Iyaku Journal. 2018;**54**:939-949 (in Japanese)

[27] Miller JM, Hair JG, Hebert M, et al. Fulminating bacteremia and pneumonia due to *Bacillus cereus*. Journal of Clinical Microbiology. 1997;**35**:504-507

[28] Tsutsumi Y. Malacoplakia and cystitis. Byori-to-Rinsho. 2010;**28**(Extra issue: Pathology Key Words):228-229

[29] Hori S, Tsutsumi Y. Histologic differentiation between chlamydial and bacterial epididymitis: Non-destructive and proliferative versus destructive and abscess-forming. Immunohistochemical and clinicopathologic findings. Human Pathology. 1995;**26**:402-407

[30] Mori M, Watanabe M, Sakuma M, Tsutsumi Y. Infectious etiology of xanthogranulomatous cholecystitis: Immunohistochemical identification of bacterial antigens in the xanthogranulomatous lesions. Pathology International. 1999;**49**:849-852

[31] Tsutsumi Y. Pathology of respiratory tract infections. Saishin Igaku Suppl: ABC of Diagnosis and Treatment 129 "Infection of the Respiratory Tract". 2017. pp. 29-56 (in Japanese)

[32] Villanueva SYAM, Saito M, Tsutsumi Y, et al. High virulence in hamsters of four dominant *Leptospira* serovars isolated from rats in Philippines. Microbiology. 2014;**160**:418-428

[33] Mahlen SD. *Serratia* infections: From military experiments to current

practice. Clinical Microbiology Reviews. 2011;**24**:755-791

[34] Takahashi J, Daa T, Gamachi A, et al. Human intestinal spirochetosis in Japan; its incidence, clinicopathologic features, and genotypic identification. Modern Pathology. 2008;**21**:76-84

[35] Tanaka Y, Matsumoto Y, Shimada N, et al. Identification and characterization of *Brachyspira aalborgi* and *Brachyspira pilosicoli* isolated from humans. Nihon Rinsho Biseibutugaku Zasshi. 2016;**26**:30-40 (in Japanese with English abstract)

[36] Horseman MA, Surani S. A comprehensive review of *Vibrio vulnificus*: An important cause of severe sepsis and skin and soft-tissue infection. International Journal of Infectious Diseases. 2011;**15**:e157-e166

[37] Snyder J, Fisher D. Pertussis in childhood. Pediatrics in Review. 2012;**33**:412-420

[38] Stelter K. Tonsillitis and sore throat in children. GMS Current Topics in Otorhinolaryngology—Head and Neck Surgery. 2014;**13**:Doc07. DOI: 10.3205/cto000110

[39] Sezer B, Akdeniz BG, Günbaya S, et al. Actinomycosis osteomyelitis of the jaws: Report of four cases and a review of the literature. Journal of Dental Sciences. 2017;**12**:301-307

[40] Shariff M, Gunasekaran J. Pulmonary nocardiosis: Review of cases and an update. Canadian Respiratory Journal. 2016;**2016**:7494202. DOI: 10.1155/2016/7494202

[41] Oshima Y, Fujii M, Shiogama K, et al. *Bartonella henselae* infection caused by cat flea bite. Pathology International. 2016;**66**:177-179

[42] Nakamura M, Kurimoto M, Kato T, Kunieda T. Cat-scratch disease presenting as a solitary splenic abscess in an elderly man. BML Case Reports. 2015 Mar 24; 2015. DOI: 10.1136/bcr-2015-209597

[43] Zhou F, Yu L-X, Ma Z-B, et al. Granulomatous lobular mastitis. Chronic Diseases and Translational Medicine. 2016;**2**:17-21

[44] Ahmed ARH, El-Badawy ZH, Mohamed IR, Abdelhameed WAM. Rhinoscleroma: A detailed histopathological diagnostic insight. International Journal of Clinical and Experimental Pathology. 2015;**8**:8438-8445

[45] Yuasa H, Ogihawa H, Fujita Y, et al. A case of rhinoscleroma in nasal cavity. Shindan Byori. 2018;**35**:206-209 (in Japanese with English abstract)

[46] Luce-Fedrow A, Lehman ML, Kelly DJ, et al. A review of scrub typhus (*Orientia tsutsugamushi* and related organisms): Then, now, and tomorrow. Tropical Medicine and Infectious Diseases. 2018;**3**(1):8. DOI: 10.3390/tropicalmed3010008

[47] Tsutsumi Y. Electron microscopic study using formalin-fixed, paraffin-embedded material, with special reference to observation of microbial organisms and endocrine granules. Acta Histochemica et Cytochemica. 2018;**51**:63-71

[48] de Lima Barros MB, de Almeida Paes R, Schubach AO. *Sporothrix schenckii* and sporotrichosis. Clinical Microbiology Reviews. 2011;**24**:633-654

[49] Prindaville B, Belazarian L, Levin NA, Wiss K. Pityrosporum folliculitis: A retrospective review of 110 cases. Journal of the American Academy of Dermatology. 2018;**78**:511-514

[50] Ono M, Nishigori C, Tanaka C, et al. Cutaneous altenariosis in an immunocompetent patient: Analysis of

the internal transcribed spacer region of rDNA and Brm2 of isolated *Alternaria alternata*. The British Journal of Dermatology. 2004;**150**:773-775

[51] Dimino-Emme L, Gurevitch AW. Cutaneous manifestations of disseminated cryptococcosis. Journal of the American Academy of Dermatology. 1995;**32**:844-850

[52] Suwabe H, Yabe H, Tsutsumi Y. Relapsing hemorrhagic varicella. Pathology International. 1996;**46**:605-609

[53] Arvin AM, Kinney-Thomas E, Shriver K, et al. Immunity to varicella-zoster viral glycoproteins, gp I (gp 90/58) and gp III (gp 118), and to a nonglycosylated protein, p 170. Journal of Immunology. 1986;**137**:1346-1351

[54] Paz C, Samake S, Anderson JM, et al. *Leishmania major*, the predominant *Leishmania* species responsible for cutaneous leishmaniasis in Mali. The American Journal of Tropical Medicine and Hygiene. 2013;**88**:583-585

[55] Kumar R, Bumb RA, Ansari NA, et al. Cutaneous leishmaniasis caused by *Leishmania tropica* in Bikaner, India: Parasite identification and characterization using molecular and immunologic tools. The American Journal of Tropical Medicine and Hygiene. 2007;**76**:896-901

[56] Lorenzo-Morales J, Khan NA, Walochnik J. An update on *Acanthamoeba* keratitis: Diagnosis, pathogenesis and treatment. Parasite. 2015;**22**:10. DOI: 10.1051/parasite/2015010

[57] Takashima Y, Kimura M, Watanabe K, et al. A case of *Acanthamoeba* keratitis with histological detection of trophozoites and cysts. Shindan Byori. 2018;**35**:54-58 (in Japanese with English abstract)

[58] Mackey-Lawrence NM, Petri WA Jr. Amoebic dysentery. Clinical Evidence. 2011;**01**:918. PMID: 21477391

[59] Saadatnia G, Golkar M. A review on human toxoplasmosis. Scandinavian Journal of Infectious Diseases. 2012;**44**:805-814

[60] Rossle NF, Latif B. Cryptosporidiosis as threatening health problem: A review. Asian Pacific Journal of Tropical Biomedicine. 2013;**3**:916-924

[61] Post L, Garnaud C, Maubon D, et al. Uncommon and fatal case of cystoisosporiasis in a non HIV-immunosuppressed patient from a non-endemic country. Parasitology International. 2018;**67**:1-3

[62] Agholi M, Aliabadi E, Hatam GR. Cystoisosporiasis-related human acalculous cholecystitis: The need for increased awareness. Polish Journal of Pathology. 2016;**67**:270-276

[63] Babb RR, Wagener S. *Blastocystis hominis*: A potential intestinal pathogen. The Western Journal of Medicine. 1989;**151**:518-519

[64] Kaneda Y, Horiki N, Cheng X-J, et al. Serologic response to *Blastocystis hominis* infection in asymptomatic individuals. The Tokai Journal of Experimental and Clinical Medicine. 2000;**25**:51-56

[65] Ligon BL. Gnathostomiasis: A review of a previously localized zoonosis now crossing numerous geographical boundaries. Seminars in Pediatric Infectious Diseases. 2005;**16**:137-143

[66] Sakanari JA, McKerrow JH. Anisakiasis. Clinical Microbiology Reviews. 1989;**2**:278-284

[67] Ishii A, Tsuji M, Tada I. History of Katayama disease: Schistosomiasis japonica in Katayama district,

Hiroshima, Japan. Parasitology International. 2003;**52**:313-319

[68] Zhou Y-B, Zheng H-M, Jiang Q-W. A diagnostic challenge for schistosomiasis japonica in China: Consequences on praziquantel-based morbidity control. Parasites Vectors. 2011;**4**:194. DOI: doi.org/10.1186/ 1756-3305-4-194

[69] Gray DJ, Ross AG, Li Y-S, McManus DP. Diagnosis and management of schistosomiasis. British Medical Journal. 2011;**342**:d2651. DOI: 10.1136/bmj. d2651

[70] Takahashi K, Uraguchi K, Kudo S. The epidemiological status of *Echinococcus multilocularis* in animals in Hokkaido, Japan. Mammal Study. 2005; **30**:S101-S105

[71] Gripper LB, Welburn SC. Neurocysticercosis infection and disease. A review. Acta Tropica. 2017; **166**:218-224

[72] Achermann Y, Goldstein EJC, Coenye T, Shirtliff ME. *Propionibacterium acnes*: From commensal to opportunistic biofilm-associated implant pathogen. Clinical Microbiology Reviews. 2014;**27**:419-440

[73] Eishi Y. Propionibacterium Acnes as a Cause of Sarcoidosis. InTechOpen (Open Access Peer-reviewed Chapter), London, U.K; 2013. DOI: 10.5772/55073

[74] Das AK. Hepatic and biliary ascariasis. Journal of Global Infectious Diseases. 2014;**6**:65-72

[75] Nagakura K, Tsutsumi Y, Moriya H, et al. Serologic findings in hepatic ascariasis: A case report. The Tohoku Journal of Experimental Medicine. 1992; **167**:121-126

[76] Bi K, Chen Y, Zhao S, et al. Current visceral leishmaniasis research: A research review to inspire future study. BioMed Research International. 2018, Article ID 9872095. DOI: 10.1155/2018/ 9872095

[77] Nagata H, Kato G, Kimura M, Okabe H. A case of kala azar. Shindan Byori. 2001;**18**:388-391 (in Japanese)

[78] Trabelsi H, Dendana F, Sellami A, et al. Pathogenic free-living amoebae: Epidemiology and clinical review. Pathologie-biologie. 2012;**60**:399-405

[79] Tsutsumi Y, Tachibana H, Azuma S, et al. Acanthoamebic meningoencephalitis associated with alcoholic liver cirrhosis. Pathology Case Reviews. 2002;**7**:273-277

[80] Jung S, Schelper RL, Visvesvara GS, Chang HT. *Balamuthia mandrillaris* meningoencephalitis in an immunocompetent patient. Archives of Pathology & Laboratory Medicine. 2004;**128**:466-468

[81] Siddiqui R, Khan NA. *Balamuthia mandrillaris*: Morphology, biology, and virulence. Tropical Parasitology. 2015;**5**: 15-22